Development of Semi-Empirical M.O. Calculation Incorporating Solvent Effect: MOMGB.

by

Makoto Harada

Department of Chemistry
Graduate School of Science
Osaka University

August, 1998

INDEX

Chapter 1 Introduction.

Many fundamental researches about a solvation have been made and now, a lot of studies are carried out in all of the branches of solution chemistry. The subject of the studies about the solvation are mainly to know what kind of parameters can characterize the property of solutions, how their values can be measured experimentally and how their values can be evaluated by the empirical procedures or theoretical calculations. However, theoretical treatments of solvation phenomena are very difficult because of the following reasons. There are a great number of molecules responsible for the solvation in the order of Avogadro's number, 6.0×10^{23} and specific solute-solvent interactions such as hydrogen bonding and charge-transfer in addition to non-specific interactions. The interactions between solvent molecules accessible to a solute molecule affects not only its property but also the network among the solvent molecules. Thus, the solute-solvent interactions are affected with each others and the information derived from experimental data could not be explained without an empirical modification using various solvation parameters. In many cases, the empirical methods matching with the experiments are convenient for analogous systems. In 1920, Born proposed the dielectric continuum model for ion solvation phenomena, which is based on an assumption that hard sphere ion is embedded in a dielectric continuum medium with the dielectric constant[1]. This Born model is very easy to use since the radius of solute molecule and the dielectric constant of the solvent are all the model requires. This model, however, does not always give considerable result. So many workers are using this model adding various modifications or expansions (see the following chapters).

Recently, the dramatic developments of computer technology enabled us to carry out complex and enormous theoretical calculations. For example, there are Molecular Orbital calculation, Molecular Mechanics calculation, Molecular Dynamics calculation, Monte Carlo simulation, and so on. These methods basically include some empirical or semi-empirical parameters or approximations and lead to the results with the condition set such as temperature, geometry (although it is optimized at last in calculation), charges, etc. using the manners based on each theory. Nevertheless, theoretical calculations for a solvation system cannot be made without a lot of facilities such as more computer power, computing time, excellent softwares, man powers for an expert and up-to-date knowledge of computing operation, and so on.

In this thesis, we expand the model made up by Born and modify it so as to apply to various solvation systems. Chapter 2 describes the application of the classic Born equation to poly-cyclic

aromatic hydrocarbon (PAH) mono-cations, the evaluation of solvation energies of PAH molecules using Generalized Born (GB) equation[2-6], as the name implies, which is a modified Born equation in order to treat poly-atomic solute molecules. It is further improved here to give Modified GB (MGB) equation and its derivation and application will be given. In Chapter 3, MGB equation introduced in Chapter 2 is expanded more to MOMGB method, which is based on semi-empirical M.O. calculation program package MOPAC Ver.6.0[7,8]. Finally, Chapter 4 describes some applications of MOMGB to experimental data such as solvation free energies and vertical ionization potentials in solution, poly-cyclic aromatic hydrocarbons in acetonitrile, alkoxide anion in water and alcohols, and bromide anion in various solvents.

References

[1] M. Born, *Z. Physik* 1 (1920) 45.

[2] G. J. Hijtink, E. de Boer, P. H. van der Meij, W. P. Weijland, *Rev. Trav. Chim. Pays-Bas* 75 (1956) 487.

[3] I. Jano, *C. R. Seances Acad. Sci.* 261 (1965) 103.

[4] O. Tapia, Quantam Theory of Chemical Reactions; R. Daudel, A. Pullman, L. Salem., A. Veillard, Eds.; Reidel: Dordrecht, 1980; Vol. II, p25.

[5] R. Constanciel, O. Tapia, *Theor. Chim. Acta* 55 (1980) 77.

[6] O. Chavlet, I. Jano, *C. R. Seances Acad. Sci.* 259 (1964) 1867.

[7] J. J. P. Stewart, *J. Comput. Chem.* 10 (1989) 209.

[8] MOPAC Ver.6.00(QCPE #455, VAX version), J.J.P. Stewart, received as Ver.6.01(JCPE P049) for UNIX-Sun SPARCstation version by Kazuhiro Nishida.

Chapter 2 Principle of the Born Equation for the Solvation free energy and Generalized Born Equation.

2.1. Introduction

In order to predict the solvation free energy ΔG_s for an ion, which is the energy of transfer of a charged molecular species from vacuum into solvent, the Born equation [1,2] is most frequently used [3] if the main concern is placed on its electrostatic interaction with solvent. The model proposed by Born in 1920 was based on that of a hard sphere ion in a dielectric continuum at an infinitely dilute concentration. Considering only electrostatic interactions the Born equation for the solvation free energy is,

$$-\Delta G_s = \frac{1}{2}\frac{e^2}{4\pi\varepsilon_0}\left(1-\frac{1}{\varepsilon_r}\right)\frac{q^2}{r}, \qquad (2.1)$$

where ε_0 is the permittivity of free space (8.854×10^{-12} $J^{-1}C^2m^{-1}$), ε is the dielectric constant of the solvent, q is the ionic charge, e is the charge of an electron, and r is the solute radius. The equation predicts that the ion solvation free energy is proportional to r^{-1}. In fact, excellent proportionality has been known for inorganic ions in aqueous solution especially when slight modification is given to the r values [4]. It also could have been used rather successfully for the systems lacking strong solute-solvent interaction such as hydrogen bonding. The Born equation, however, has long been known to be inadequate to predict experimental solvation free energies.

In the present system the solute ions are polycyclic aromatic hydrocarbon(PAH) mono-cations and the solvent is acetonitrile. Therefore, there should not exist any specific solute-solvent interactions and the Born equation must be applicable. However, it is our finding that the solvation energy for mono-cation of planar molecule is proportional to r^{-2}. Such dependence upon r^{-2} has also been reported recently by Osakai and coworkers for polymeric molybdates [5]. In this chapter paper a new simple method is proposed to predict solvation energies of PAH mono-cations, which is derived by modifying the generalized Born equation.

2.2. Experimental Solvation Energy Data

The total free energy change, ΔG_s^{stat}, associated with the transfer of a PAH cation from vacuum into acetonitrile, as determined from the Born-Haber thermodynamic cycle shown in Figure 2.1, is equal to the sum of the following fractional energy changes:

(1) the energy of discharging the cation in vacuum, $-I_p$ (I_p is the ionization potential).

(2) the energy of transferring the neutral PAH molecule from vacuum into acetonitrile, ΔG_n, which is the solvation free energy of the neutral PAH molecule.

(3) the energy of recharging the transferred neutral PAH molecule in acetonitrile, which corresponds to the standard oxidation potential E_{ox}° .

where ΔG_H is the transfer energy of an electron from vacuum to N.H.E. [6]. It is considered here

$$\Delta G_s = -I_p + \Delta G_n + E_{ox}^{\circ}(\text{vs. N.H.E.}) - \Delta G_H, \qquad \textbf{(2.2)}$$

that (ΔG_s - ΔG_n) leaves only the electrostatic interaction energy, ΔG_s^{stat}, since the other energies contributing to the solvation, e.g., cavity-formation in solvent and the van der Waals solute-solvent interaction, must be similar for the cation and neutral states. That is,

$$-\Delta G_s^{stat} = -(\Delta G_s - \Delta G_n) = I_p - E_{ox}^{\circ}(\text{vs. N.H.E.}) - 4.5\text{eV}. \qquad \textbf{(2.3)}$$

This is true for larger molecules with delocalized charge distribution for cation state. The E_{ox}° values in acetonitrile are collected from the report by Parker et al. [7]. Essentially the same values have also been reported by Kubota and co-workers [8] and many others(the references to Table 1). Since the electrochemical oxidations of benzene and some others are of irreversible reaction, their E_{ox}° values are the estimated ones, thus containing some uncertainties.

Parker also calculated the ΔG_s^{stat} using theoretical I_p by the MO calculation and experimental E_{ox}° values. He concluded that from benzene to perylene the cation solvation energies are the same [7,9]. The conclusion, the independence of solvation energy on the molecular size, is strange to be true and in fact one can find some differences in ΔG_s^{stat} energies among the aromatic molecules if the experimental I_p values are used instead of the values calculated with the MO theory.

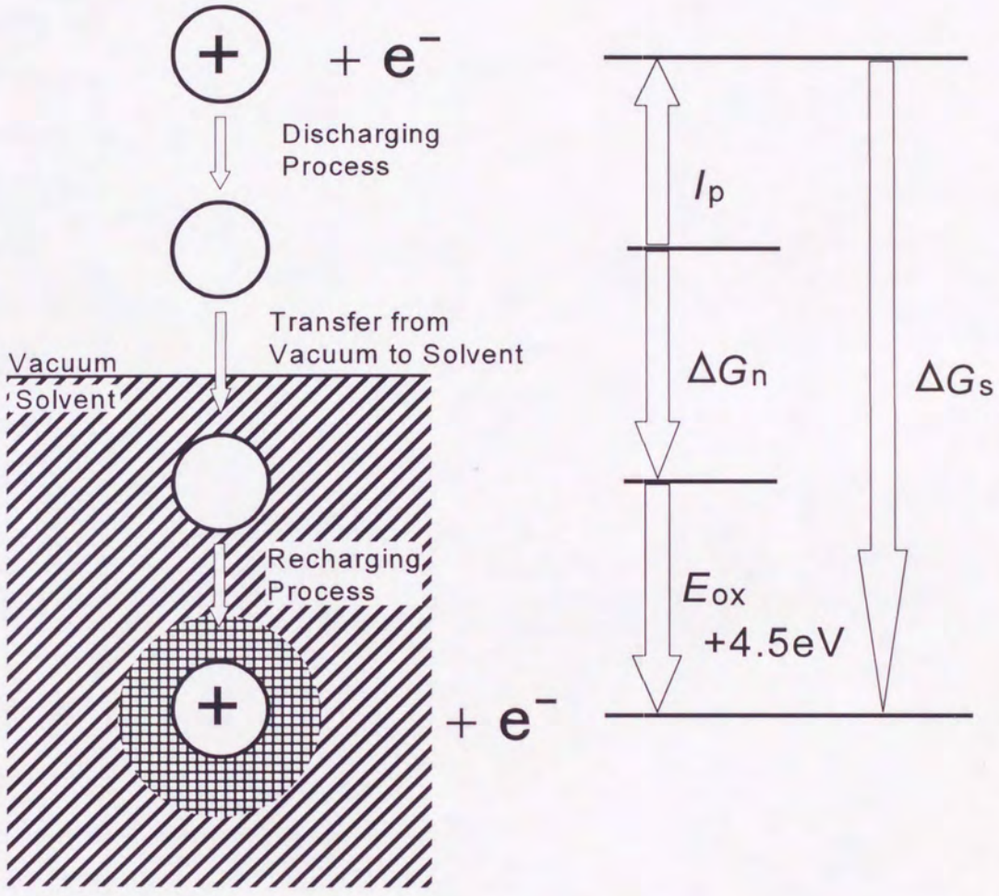

Fig. 2.1. Born-Haber thermodynamic cycle for mono-cation solvation.

In Table 2.1 are collected the I_p data by the high resolution photoelectron spectroscopy. The use of the reliable experimental I_p values leads to the reasonable trend in solvation energy, i.e., the larger the cation molecule, the smaller the solvation energy.

TABLE 2.1. Ionization potential I_p, oxidation potential E^o in acetonitrile vs. N.H.E., electrostatic interaction energy ΔG_s^{stat} in acetonitrile for polycyclic aromatic hydrocarbons.

molecule	E^o_{ox} /V	I_p /eV	$-\Delta G_s^{stat}$ /eV
benzene	2.82[a],2.86[b]	9.24[d]	1.92
naphthalene	2.06[a]	8.15[d]	1.59
anthracene	1.61[a],1.56[c]	7.43[e]	1.32
phenanthrene	2.02[a]	7.87[f]	1.35
triphenylene	2.07[a]	7.88[d]	1.31
pyrene	1.68[a],1.52[c]	7.41[g]	1.23
benz[a]anthracene	1.70[a],1.63[c]	7.41[d]	1.21
benzo[a]pyrene	1.40[c]	7.12[h]	1.22
perylene	1.37[a],1.28[c]	6.97[g]	1.10
benzo[e]pyrene	1.79[a]	7.43[i]	1.14
chrysene	1.87[a],1.83[c]	7.59[d]	1.22
benzo[b]triphenylene	1.77[a]	7.39[d]	1.12
benzo[a]chrysene	1.85[a]	7.51[d]	1.16
dibenz[a,h]anthracene	1.71[a],1.67[c]	7.38[d]	1.17
coronene	1.75[a],1.59[c]	7.34[g]	1.09
benzo[b]chrysene	1.53[a]	7.20[d]	1.17
dibenz[a,j]anthracene	1.78[a]	7.40[d]	1.12
naphthacene	1.29[a],1.22[c]	6.97[d]	1.18

[a]Reference 7. [b]J.O. Howell, J.M. Goncalves, C. Amatore, L. Klasinc, R.M. Wightman, J.K. Kochi, *J. Am. Chem. Soc.* 106 (1984) 3968. [c]Reference 8. [d]W. Schmidt, *J. Chem. Phys.* 66 (1977) 828. [e]L. Klasinc, B. Kovac, S. Schoof, H. Guesten, *Croat. Chem. Acta* 51 (1978) 307. [f]N.S. Hush, A.S. Cheung, P.R. Hilton, *J. Electron Spectrosc. Relat. Phenom.* 7 (1975) 385. [g]E. Clar, W. Schmidt, *Tetrahedron* 32 (1976) 2563. [h]I. Akiyama, K.C. Li, P.R. LeBreton, P.P. Fu, R.G. Harvey, *J. Phys. Chem.* 83 (1979) 2997. [i]R. Boschi, E. Clar, W. Schmidt, *J. Chem. Phys.* 60 (1974) 4406.

3.3. r^{-2} Dependence of Solvation Energy

At first, the applicability of the Born equation to the solvation energies of the PAH cations is tested. According to the Born equation, ΔG_s^{stat} is proportional to r^{-1}. Here the radii of the cations are estimated from their densities d as follows,

$$r_d = \frac{1}{2}\left(\frac{M_W}{N_A d}\right)^{\frac{1}{3}}, \qquad \textbf{(2.4)}$$

where M_W is the molecular weight and N_A is the Avogadro's number.

The ΔG_s^{stat} values are calculated by using eq.1 with $\varepsilon_r = 35.94$ and $q = +1$. In Figure 2 are compared the ΔG_s^{stat} values with r_d^{-1}. It is clearly shown that the extrapolation of the plot to $r_d^{-1} = 0$ gives non-zero ΔG_s^{stat} value. If it is remembered that the infinitely large ion (with the charge evenly spread over the ion) should have no electrostatic interaction energy, the plot must be a part of a curve which reaches the origin of the graph. Since the ions used here are not spherical, thus the applicability of the Born equation with the r_d value should be limited.

However, it is quite interesting to find that the dependence of ΔG_s^{stat} on r_d^{-1} is not linear but quadratic. The ΔG_s^{stat} value vs. r_d^{-2} plot is included in Figure 2.2. In the figure, the abscissa scale is normalized at benzene. Even if the points of benzene and naphthalene are omitted from the figure since they have some uncertainties in E_{ox}°, the figure still indicates that ΔG_s^{stat} is rather proportional to r_d^{-2} than r_d^{-1}. The conclusion is possible to be reversed if the potential of the reference electrode and/or the ΔG_H value were in error of more than 1eV. However, it is highly unlikely and we presume that the error is less than 0.2 - 0.3eV at maximum.

Since r_d^2 has the dimension of area, the present result may suggest that the ion solvation energy is inversely proportional to the surface charge density, the charge per unit surface area on the ion.

Instead of collecting the experimental density data one can estimate the r values from the volume V, which is calculated from the very simple molecular model as shown in Figure 2.3. It is composed of hexagonal boxes having the height of 3.4 Å, i.e. carbon atom diameter. Hydrogens are given the radius of 1.2 Å. Figure 2.3 again indicates the correlation of ΔG_s^{stat} with $V^{-2/3}$, which has the dimension inverse of area. Some of the points are added in Figure 2.3 which are missing in Figure 2.2 owing to the lack of density data.

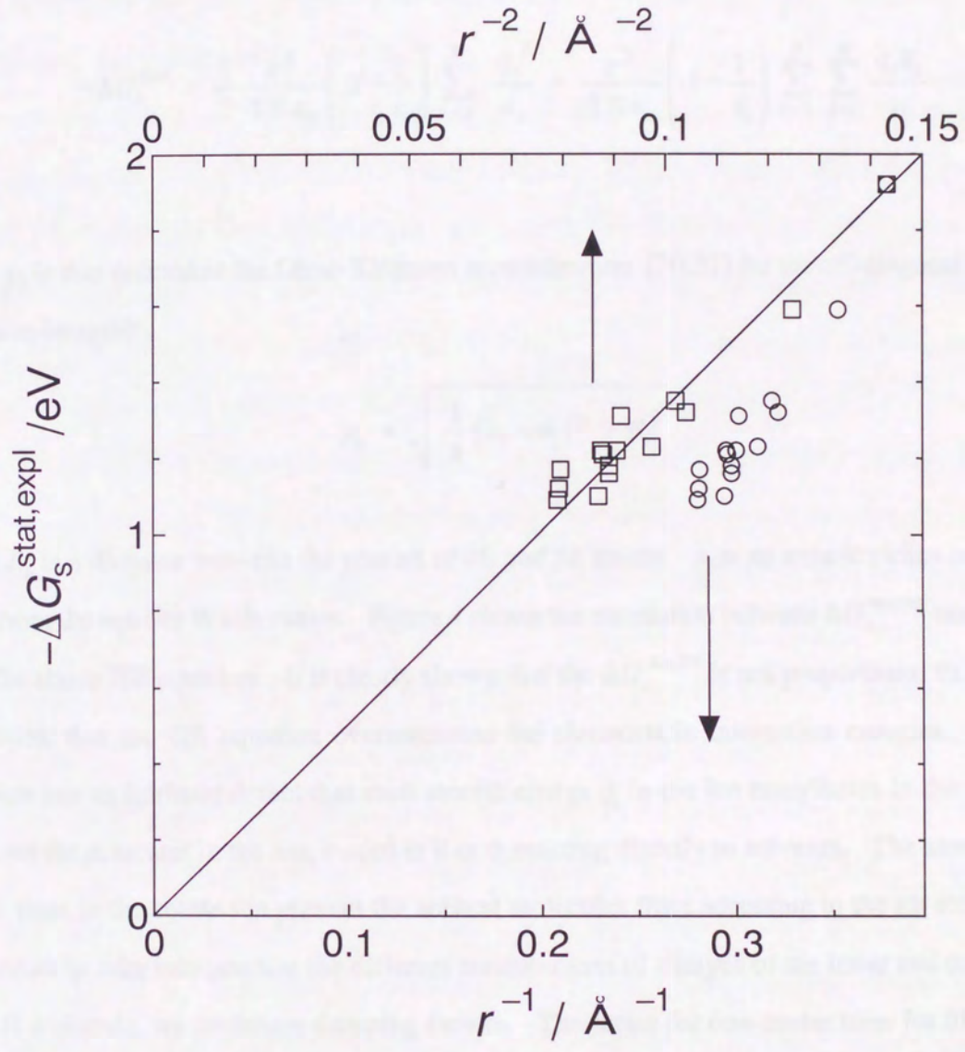

Fig. 2.2. The correlation between $\Delta G_s^{stat,expl}$ and r_d^{-1} and r_d^{-2} for PAHs.

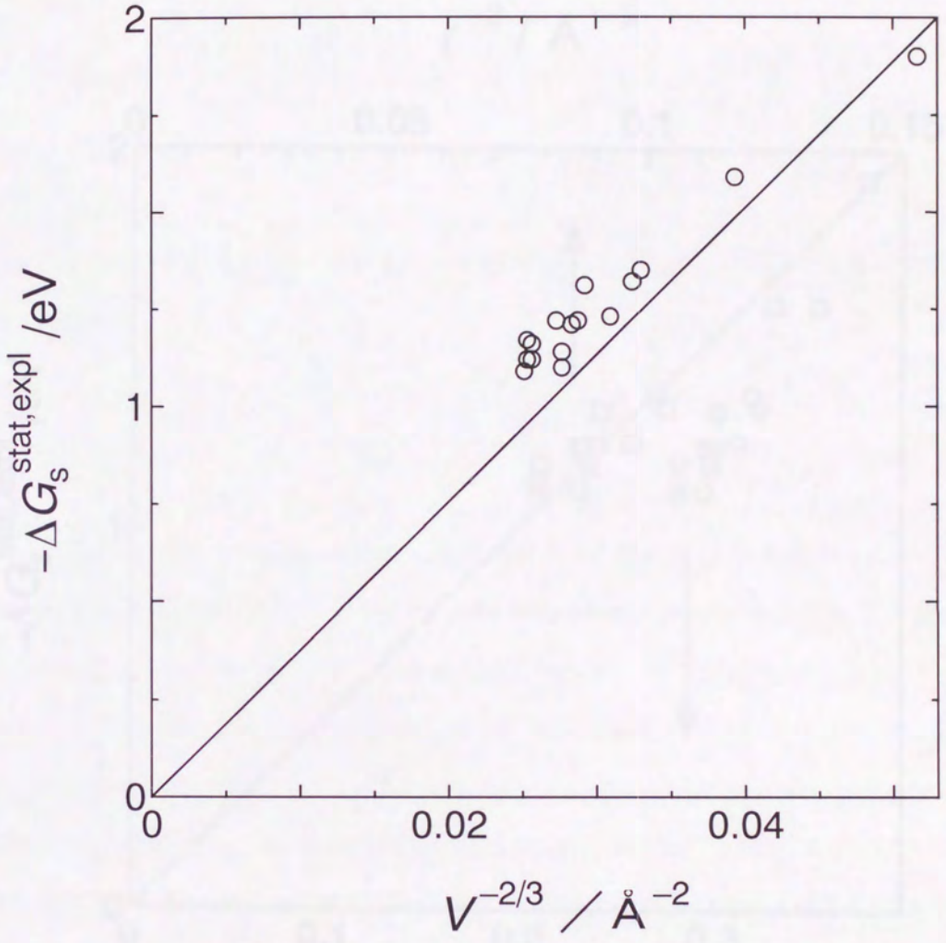

Fig. 2.3. The correlation between $\Delta G_s^{stat,expl}$ and $V^{-2/3}$ for PAHs. Inserted is a polygonal box model for calculating the V value of benzene as an example.

2.4. Generalized Born Equation

The r^{-2} dependence of solvation energy has been found for polymeric molybdates by Osakai and co-workers [5,10]. They discussed the dependence in terms of surface charge density-dielectric solvent interaction and they considered the interaction as being due to partial charge transfer from the polymeric molybdates to solvent [5].

Here we try to obtain the r^{-2} dependence within the Born theory. Even Born had predicted the values of solvation free energies far from those observed experimentally, with errors greater than 50% [1]. Therefore, the Born equation has been modified by many investigators in order to predict their experimental data that could not be interpreted using the basic Born equation. Latimer et al. focused their discussion on the radius of the solute ion [11]. They adopted the ionic radii which reproduced experimental values. Those values are obtained by adding 0.85 and 0.1 Å for anions to crystal radii of alkali metal cations and univalent anions in water, respectively. Stokes used a van der Waals radius [12]. Raschin adjusted the ionic radius so as to achieve agreement between theoretical and experimental values for a variety of cations and anions. Other investigators paid attention to the dielectric constant of the solvent. The Born equation assumes that the dielectric constant is uniform. However, it has been generally recognized that under the presence of the strong solute-solvent interaction, the solvent dipoles must be aligned and the dielectric constant of the solvent surrounding the solute ion be lower. So, Noyes calculated the solvation free energy with an effective dielectric constant which was lower than that in the bulk solvent [13]. Abraham et al. proposed that a layered solvent model in which each layer has specified thickness and relative permittivity [14 - 17]. They were adjusted in order to reproduce the experimental values. Laider et al. [18] and Markin et al. [19] used simplified or asymptotic forms of the Booth equation [20] to describe the relationship between the high electric field and low solvent permittivity which lead to the dielectric saturation effects in the calculation of the solvation free energies. In addition, Bontha et al. proposed that dielectric saturation effects could be estimated using the modified Laplace equation for the electric potential in a polarizable dielectric medium, the Booth equation for the variation in the solvent permittivity with electric field strength and the Goldschmidt radius with the error less than 10% [21].

In those previous studies, the solute ions treated were often mono-atomic ions. For poly-atomic

molecules the generalized Born (GB) equation has been given by Hoijtink and coworkers [22] and Chalvet and Jano [23,24]. Solvation free energy [25,26], solvent effect [27,28], and reaction mechanism [28,29] have also been studied using the GB equation. They derived the following GB equation for ΔG_s^{stat} from the combination of Coulomb's law and the Born equation,

$$-\Delta G_s^{stat} = \frac{1}{2}\frac{e^2}{4\pi\varepsilon_0}\left(1-\frac{1}{\varepsilon_r}\right)\sum_{i=1}^{N}\frac{q_i^2}{a_i} + \frac{e^2}{4\pi\varepsilon_0}\left(1-\frac{1}{\varepsilon_r}\right)\sum_{i=1}^{N}\sum_{j<i}^{N}\frac{q_i q_j}{\gamma_{ij}} \qquad \textbf{(2.5)}$$

where γ_{ij} is that defined as the Ohno-Klopman approximation [30,31] for the off-diagonal Coulomb repulsion integrals,

$$\gamma_{ij} = \sqrt{\frac{1}{4}(a_i + a_j)^2 + R_{ij}^2} \qquad \textbf{(2.6)}$$

where R_{ij} is a distance between the centers of *i*th and *j*th atoms. a_i is an atomic radius of *i*th atom taken from the van der Waals radius. Figure 4 shows the correlation between $\Delta G_s^{stat,expl}$ and $\Delta G_s^{stat,GB}$ from the above GB equation. It is clearly shown that the $\Delta G_s^{stat,GB}$ is not proportional to $\Delta G_s^{stat,expl}$. We think that the GB equation overestimates the electrostatic interaction energies. The GB equation has an intrinsic defect that each atomic charge q_i in the ion contributes in the same way wherever the q_i locates in the ion, buried in it or contacting directly to solvents. The atoms around the *i*th atom in the solute ion prevent the solvent molecules from accessing to the *i*th atom.

In order to take into account the different contributions of charges of the inner and outer atoms in PAH molecule, we introduce dumping factors. The factor for one-center term for *i*th atom, L_i, is obtained from the distance between the center of *i*th atom and the nearest point on the molecular ion-solvent. Here we adapted the effective radius of H atom, 1.2 Å, which is its van der Waals radius. For the Coulomb repulsion integral term, the dumping factor, L_{ij}, is defined to be a distance from the center between *i*th and *j*th atoms to the nearest point on the molecular boundary. The GB equation is now modified as follows,

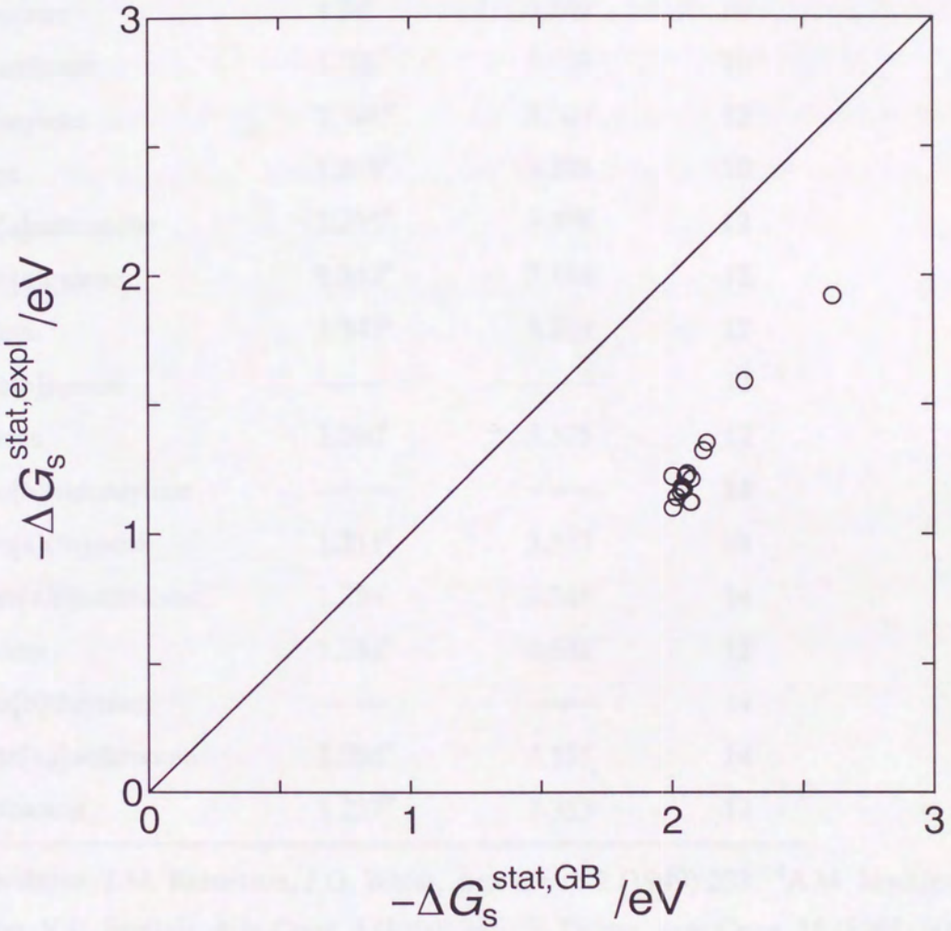

Fig. 2.4. The correlation between $\Delta G_s^{stat,expl}$ and $\Delta G_s^{stat,GB}$ from GB equation.

TABLE 2.2. Density d, radius by cubic approximation r, and the number of hydrogens in the polycyclic aromatic hydrocarbon N_H.

molecule	d /g·cm^{-1}	r /Å	N_H
benzene	0.879	2.643	6
naphthalene	1.172[j]	2.832	8
anthracene	1.24[k]	3.102	10
phenanthrene	1.203[l]	3.133	10
triphenylene	1.308[m]	3.309	12
pyrene	1.275[n]	3.206	10
benz[a]anthracene	1.232[o]	3.376	12
benzo[a]pyrene	1.352[p]	3.384	12
perylene	1.341[q]	3.393	12
benzo[e]pyrene	——	——	12
chrysene	1.290[r]	3.325	12
benzo[b]triphenylene	——	——	14
benzo[a]chrysene	1.311[s]	3.353	14
dibenz[a,h]anthracene	1.294[t]	3.548	14
coronene	1.381[u]	3.561	12
benzo[b]chrysene	——	——	14
dibenz[a,j]anthracene	1.286[v]	3.555	14
naphthacene	1.257[w]	3.353	12

[j]S.C. Abrahams, J.M. Robertson, J.G. White, *Acta Cryst.* 2 (1949) 233. [k]A.M. Mathieson, J.M. Robertson, V.C. Sinclair, *Acta Cryst.* 3 (1950) 245. [l]J. Trotter, *Acta Cryst.* 16 (1963) 605. [m]F.R. Ahmed, J. Trotter, *Acta Cryst.* 16 (1963) 503. [n]A. Camerman, J. Trotter, *Acta Cryst.* 18 (1965) 636. [o]P.H. Friedlander, D. Sayre, *Nature* 178 (1956) 999. [p]J. Iball, D.W. Young, *Nature* 177 (1956) 985. [q]D.M. Donaldson, J.M. Robertson, J.G. White, *Proc. Roy. Soc.* (London) A220 (1953) 311. [r]D.M. Burns, J. Iball, *Proc. Roy. Soc.* (London) A257 (1960) 491. [s]A. De, R. Ghosh, S. Roychowdhury, P. Roychowdhury, *Acta Crystallogr. Sert. C: Cryst. Struct. Commun.* C41 (1985) 907. [t]J.M. Robertson, J.G. White, J. Chem. Soc. (1947) 1001. [u]J.M. Robertson, J.G. White, *Nature* 154 (1944) 605. [v]R. Kuroda, *J. Chem. Soc. Perkin Trans.* 2 (1982) 789. [w]J.M. Robertson, V.C. Sinclair, J. Trotter, *Acta Cryst.* 14 (1961) 697.

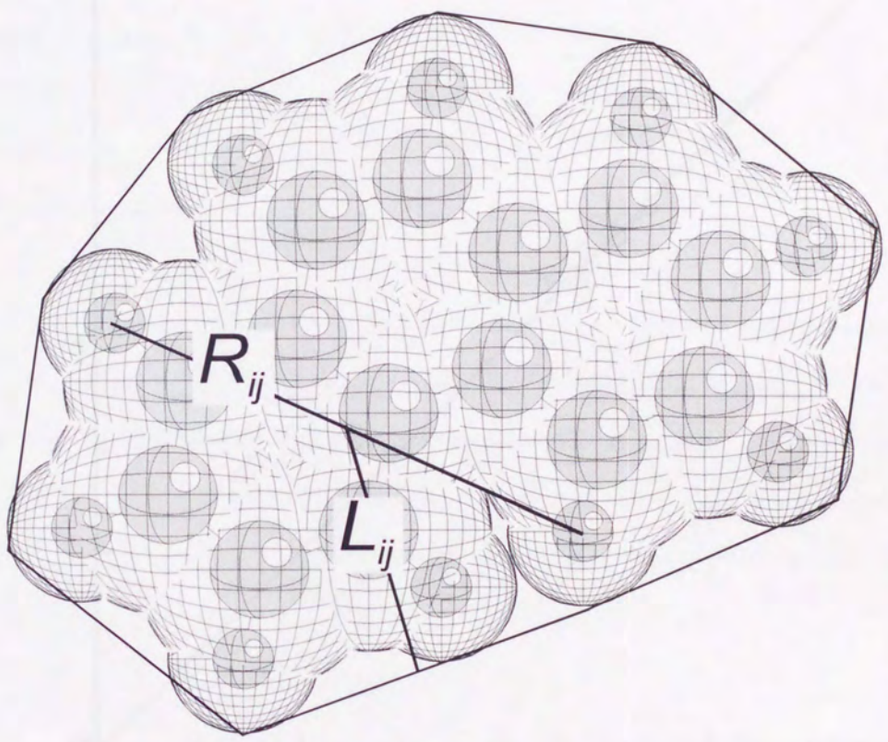

Fig. 2.5. The definitions of R_{ij} and L_{ij} for phenanthrene.

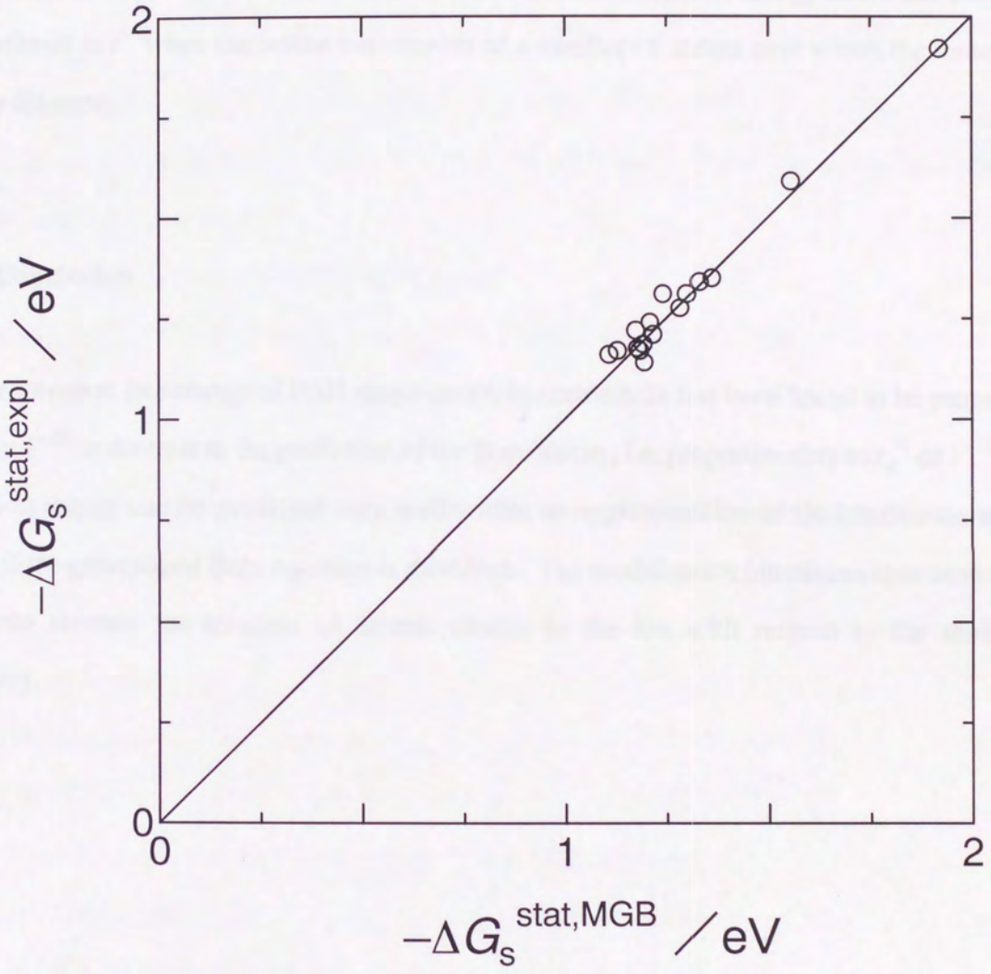

Fig. 2.6. The correlation between $\Delta G_s^{stat,expl}$ and the $\Delta G_s^{stat,MGB}$ value from the MGB equation with $q_H=N_H^{-1}$ and $q_C=0$.

This is the same conclusion as that by Osakai and co-workers for polymeric molybdates [5,10]. The structure of polymeric molybdates is almost taken up by close-packed oxygens, so the volume of the ion depends on the number of oxygen atoms, n. Assuming that the polymeric molybdates is spheric with radius r, r should be proportional to $n^{1/3}$. They then found that the standard ion-transfer energy linearly depended on $n^{-2/3}$, and concluded therefore that the solvation free energy of the polymeric molybdates linearly depends on r^{-2}. It seems that the solvation free energy of the ion tends to be proportional to r^{-2} when the solute ion consists of a number of atoms over which the ionic charge evenly disperse.

2.5. Conclusion

The solvation free energy of PAH mono-cation in acetonitrile has been found to be proportional to r_d^{-2} or $V^{-2/3}$ in contrast to the prediction of the Born theory, i.e. proportionality to r_d^{-1} or $V^{-1/3}$. The solvation energy can be predicted very well within an approximation of the continuous medium model if the generalized Born equation is modified. The modification introduces new terms which take into account the location of atomic charge in the ion with respect to the ion/solvent boundary.

2.6. References

[1] M. Born, *Z. Phys.* 1 (1920) 45.

[2] P.W. Atkins, A.J. MacDermott, *J. Chem. Edu.* 59 (1982) 5.

[3] T. Kozaki, K. Morihashi, O. Kikuchi, *J. Am. Chem. Soc.* 111 (1989) 1547.

[4] J.O'M. Bockris, A.K.N. Reddy, Modern Electrochemistry 1, Plenum Press, New York, 1970, p.70.

[5] T. Osakai, S. Himeno, A. Saito, *J. Electroanal. Chem.* 360 (1993) 299.

[6] R. Parsons in A.J. Bard, R.Parsons, J. Jordan (Eds.), Standard Potentials in Aqueous Solution, Dekker, New York, 1985, p.19.

[7] V.D. Parker, J.Am. Chem. Soc. 98 (1976) 98.

[8] T. Kuroda, K. Kano, B. Uno, T. Konse, *Bull. chem. Soc. Jpn.* 60 (1987) 3865.

[9] V.D. Parker, *J. Am. Chem. Soc.* 96 (1974) 5656.

[10] T. Osakai, S. Himeno, A. Saito, *Rev. Polarogr.* (Kyoto), 36 (1990) 61.

[11] W.M. Latimer, K.S. Pietzer, C.M. Slansky, *J. Phys. Chem.* 7 (1939) 108.

[12] R.H. Stokes, *J. Am. Chem. Soc.* 86 (1964) 979.

[13] R.M. Noyes, *J. Am. Chem. Soc.* 84 (1962) 513.

[14] M.H. Abraham, J. Lizzi, *J. Chem. Soc. Faraday Trans. 1* 74 (1978) 1604.

[15] M.H. Abraham, J. Lizzi, *J. Chem. Soc. Faraday Trans. 1* 74 (1978) 2858.

[16] M.H. Abraham, J. Lizzi, E. Kristof, *Aust. J. Chem.* 35 (1982) 1273.

[17] J. Lizzi, L. Meszaros, J. Ruff, *J. Chem. Phys.* 70 (1979) 2491.

[18] K.J. Laider, C. Pegis, *Proc. R. Soc. London* A155 (1957) 80.

[19] V.S. Markin, A.G. Volkov, *J. Electroanal. Chem.* 235 (1987) 23.

[20] F. Booth, *J. Chem. Phys.* 19 (1951) 391.

[21] J.R. Bontha, P.N. Pintauro, *J. Phys. Chem.* 96 (1992) 7778.

[22] G.J. Hoijtink, E. de Boer, P.H. van der Meij, W.P. Weijland, *Recl. Trav. Chim. Pays-Bas* 75 (1956) 487.

[23] O. Chalvet, I. Jano, *C. R. Seances Acad. Sci.* 269 (1964) 1867.

[24] J. Jano, *C. R. Seances Acad. Sci.* 261 (1965) 103.

[25] R. Cnstanciel, R. Constreras, *Theor. Chim. Acta* 65 (1984) 1.

[26] W.C. Still, A. Tempczyk, R.C. Hawley, T. Hendricson, *J. Am. Chem. Soc.* 112 (1990) 6127.

[27] T. Kozaki, K. Morihashi, O. Kikuchi, *J. Mol. Struct.* 168 (1988) 265.

[28] T. Kozaki, K. Morihashi, O. Kikuchi, *J. Am. Chem. Soc.* 111 (1986) 1547.

[29] S.C. Tucker, D.G. Truhler, *Chem. Phys. Lett.* 157 (1989) 164.

[30] K. Ohno, Theor. *Chim. Acta* 2 (1964) 219.

[31] G. Klopman, *J. Am. Chem. Soc.* 86 (1964) 4550.

[32] J.J.P. Stewart, *J. Comput. Chem.* 10 (1989) 221.

[33] MOPAC Ver.6.00(QCPE #455, VAX version), J.J.P. Stewart, received as Ver.6.01(JCPE P049) for UNIX-Sun SPARCstation version by Kazuhiro Nishida.

Chapter 3 The Introduction of Modified Generalized Born Equation into MOPAC

3.1. Introduction

Computer technology is growing rapidly. With the advance of computer technology, computational chemistry is drastically improving. There are many methods in the field of the computational chemistry such as Molecular Orbital (M.O.) theory, Molecular mechanics (MM) theory, Molecular Dynamics (MD) theory, Monte Carlo simulation (MC) theory, and so on. However, almost all of them which have been programed in order to calculate the characteristic values about various molecular systems by using these methods would require a powerful computer. Now, the price of computers has been getting down more and more, and so many investigators can utilize their computer not only in making their experiment but also in doing the simulation of their experimental data and expounding the experimental values theoretically.

When the state of a solvated molecule is closely examined, MD or MC method is often used. MD method deals with a lot of molecules in a cell and calculates the interactions between bonded and non-bonded atoms of the molecules. The configuration obtained in MD calculation is due to the interactions between their molecules and the thermal mobility of the molecules. MD calculation sets the various arrangement and the motions of the molecules in the cell according to their kinetic and potential energies and searchs for the most stable configurations. MD method is useful for a solvation investigation such as the solvation structure but difficult for the calculation of the thermal data of a solvated molecule such as solvation free energy since the energy calculated by MD methods is the internal energy and some perturbation treatment is required for the calculation of the free energy. MD thermal data in a system cannot be simply compared with that in another system. Furthermore, when the change in energy of solute molecule from one state to another is mainly governed by electrostatic interaction, the results obtained from MD calculation is not always reasonable as MD calculation uses simple potential functions with empirical parameters. Though usual MD method has the tendency as described above, it is possible to improve MD program with the parameters taking into account the electrostatic interactions in various conditions sufficiently.

Usual M.O. method can calculate various thermodynamic values in vacuum, but cannot calculate the values about a solvation. In M.O. calculation process, the charge distribution and the potential

of a molecule or a cluster complised of a few molecules play mainly important roles and the energy of the system is drastically affected by the changes in the electrostatic interaction. Solvation data could be obtained by the M.O. calculation if all of the molecules in a solution could be considered in the M.O. calculation. To accomplish this calculation, however, a number of molecules in the order of Avogadro's number, 6.0×10^{23} must be dealt with by M.O. calculation. Thus, it cannot be put to practical use. (In the future, M.O. calculation might be able to do this by a much more powerful computer than that now available.)

Then, some approaches based on the M.O. method were created to treat the solvation data theoretically. The most usual way in which the solute-solvent interactions are taken into account by M.O. calculation is to use a dielectric continuum model proposed by Born[1]. In this model, the dielectric medium is laid on the environment of a solute molecule instead of many solvent molecules surrounding a solute molecule. There are some approaches how to deal with this continuum medium. The approach of Tomasi et al [2-6] and Luque et al.[7-11] is that the solute molecule forms a cavity within the dielectric medium and its dielectric medium affects the charge density on the solvent accessible surface (SAS) as its cavity surface is the interface between the cavity and the dielectric medium. They combined the perturbed term due to this effect with M.O. calculation program such as AMPAC[12] which is the semi-empirical M.O. calculation program package. Their approach leads to a double iterative procedures on a SCF process. One is to calculate the charge distribution in vacuum is calculated (usual M.O. calculation process) and the other is that the new charge distribution which is affected by the dielectric medium on the SAS is calculated. As a result, the number of iterative calculations increases in the SCF cycle and it becomes difficult to deal with the geometry optimization. Hoshi et al.[13] assumed that the dielectric medium is inhomogeneous and a solute molecule is surrounded by more than two polarizable dielectric media having different dielectric constants. There are interactions between the molecular cavity and its contact dielectric medium or between dielectric media contacting each other through arbitrary shaped boundaries. The charge distribution of solute molecule and the dielectric constants of the media are varied due to their interaction. They developed a solution of a Green function for the dielectric media and added this solution to the hamiltonian of M.O. calculation. This approach is very

interesting and applicable to various systems. However, it is difficult to determine the boundaries among the media with different dielectric constants each other. Klampt et al. simplified the idea of Hoshi et al. of the inhomogeneous dielectric media using the homogeneous dielectric medium with a single dielectric constant[14]. They regarded the dielectric medium as a conductor and dealt with it like Onsager's solution for the screening effect[15]. Their approach is called 'Conductor-like Screening Model' or COSMO and combined with the M.O. calculation program package MOPAC93[16] as COSMO method.

The approaches of Truhlar et al.[17-20], Still et al.[21] and many other workers[22-31] to include the dielectric medium effect are based on Born type model. Still et al. applied generalized Born (GB) model[25-27, 32,33] using molecular mechanics[34,35]. GB model was developed for a poly-atomic molecule, while Born model is that for a mono-atomic molecule. Truhlar et al. combined the GB model with Austin Model 1 (AM1) method[36] in semi-empirical M.O. program package AMPAC[12]. Truhlar et al. dealt with the GB term as a perturbation term for Fock operator. A critical difference from the most previous works in which solvent effects are incorporated in the Fock operator for SCF calculations is that their treatment includes mutual solute-solvent polarization effects of the solute-induced reaction fields. In the Truhlar's method, the above approaches such as Hoshi et al. or Klampt et al. were incorporated into M.O. calculation by introducing the perturbation term for charge distribution on the SAS. Furthermore, Truhlar et al. considered the non-electrostatic term dues to the contribution of cavity formation in the solution and the solute-solvent dispersion interactions. It's limitation, however, is that their program, called AMSOL[37], can be applied only to the aqueous solutions because the parameter set used by AMSOL has been obtained from a data set consisting of aqueous solutions.

Then, the M.O. calculation program is required which is applicable to wider solution systems. They can be either an ab initio method or semi-empirical method. While the advances in ab initio method are dramatic with chemical accuracy, especially for small molecules, the advances in semi-empirical method are also rapid. The usefulness of ab initio techniques has been closely tied to the availability of well-tested general basis sets and widely applicable computer programs with analytic gradient techniques for stationary point analysis. On the other hands, the revolution in usefulness

of semi-empirical computational techniques has been closely tied to well-tested general parameterizations, such as MOPAC-PM3 (parametric method 3)[38], and to widely available general computer programs with efficient stationary point analyses. Here, we adopted semi-empirical method, MOPAC-PM3. MOPAC[39] is a package of semi-empirical M.O. calculation program like MINDO (modified intermediate neglect of differential overlap)[40], MNDO (modified neglect of diatomic overlap)[41], AM1 (Austin model 1)[36] and PM3 (parametric method 3)[38]. PM3 based on MNDO has a parameter set that has been exhaustively optimized by Stewart as the name "parametric" implies. The parameter set considers the effect of hydrogen bonding such as N···H and O···H bonding. As a result, the errors in the calculated heat of formation become smaller than that of the methods except PM3 in MOPAC without losing chemical accuracy in other parameters such as geometry, dipole moment, ionization potential, etc.[38] and, what is better, PM3 calculation is faster than the other.

This thesis presents the calculation of solvation free energies based on a treatment of continuum solvent and the semiempirical M.O. theory for atomic charges on solute molecule. The modified generalized Born (MGB) model is based on the polarization effects that dominate solvation free energies of polar and charged solutes. The self-consistent-field (SCF) approach is used to calculate the solvation effects, and it is closely related to the solvation model, the self-consistent reaction field theory, and other similar methods. The present approach has several advantages. It allows the prediction of substituent effects and the treatment of solvent-included charge recognization. The geometry of a solvated molecule is predicted from the gradient due to the solvation effect. Of course, not only the geometry but also the charge distribution, dipole moment, total energy, and the other calculated parameters must affected by the solvation.

3.2. MGB equation

In chapter 2, the term L_i is introduced as the distance between the center of ith atom and the nearest point on the ion-solvent interface on hydrogrn atom. The term L_i is evaluated by a simple

method, but it performs well in predicting explain experimental results. However, the applicability of the term L_i in chapter 2 is limited to PAH molecules as a matter of course. Then we must expand the role of term L_i in order to apply MGB equation not only to PAH molecules in acetonitrile but also to any other solute molecules in various solvents. First, the meaning of Born equation, as the base of MGB equation, is closely examined.

A radius used by MGB equation, named MGB radius here, is determined as follows. Let L_{ik} be the distance from the center of *i*th atom to the surface of solute-solvent interface in the direction of unit vector $\boldsymbol{e}_k$ as shown in Fig.3.1. If the micro-space $\mathrm{d}\tau_{rk}$ indicated by the vector $\boldsymbol{r}_k$ ($=r_k\boldsymbol{e}_k$) is apart of the dielectric medium with a permittivity $\varepsilon(\boldsymbol{r}_k)$, the Born energy u_{ik} is

$$u_{ik}(r_k, \varepsilon(\boldsymbol{r}_k)) = \frac{1}{2}\frac{q_i^2 e^2}{(4\pi)^2 \varepsilon(\boldsymbol{r}_k)}\frac{1}{r_k^4}\mathrm{d}\tau_{rk}, \tag{3.1}$$

and since $\mathrm{d}\tau_{rk}=r_k^2 \mathrm{d}r_k \mathrm{d}\Omega \mathrm{d}\Theta$,

$$u_{ik}(r_k, \varepsilon(\boldsymbol{r}_k)) = \frac{1}{2}\frac{q_i^2 e^2}{(4\pi)^2 \varepsilon(\boldsymbol{r}_k)}\frac{1}{r_k^2}\mathrm{d}r_k \mathrm{d}\Omega \mathrm{d}\Theta. \tag{3.2}$$

Here, the region along the vector $L_{ik}\boldsymbol{e}_k$ is inside of the solute molecule and no affects from the solvent medium exist in this region. The dielectric medium outside has the dielectric constant ε, then the contribution $u_{ik}(\varepsilon)$ in the direction of the unit vector $\boldsymbol{e}_k$ is

$$\begin{aligned} u_{ik}(\varepsilon) &= \frac{1}{2}\frac{q_i^2 e^2}{(4\pi)^2}\mathrm{d}\Omega \mathrm{d}\Theta \int_{L_{ik}}^{\infty}\frac{1}{\varepsilon(\mathbf{r}_k)}\frac{1}{r_k^2}dr_k \\ &= \frac{1}{2}\frac{q_i^2 e^2}{(4\pi)^2 \varepsilon}\frac{\mathrm{d}\Omega \mathrm{d}\Theta}{L_{ik}} \end{aligned}. \tag{3.3}$$

When the integral of the above equation about *k* is carried out over all the space,

$$u_i(\varepsilon) = \frac{1}{2}\frac{q_i^2 e^2}{(4\pi)^2 \varepsilon}\int \frac{\mathrm{d}\Omega\,\mathrm{d}\Theta}{L_{ik}} = \frac{1}{2}\frac{q_i^2 e^2}{4\pi\varepsilon}\lim_{k\to\infty}\sum_k \frac{1}{L_{ik}} \tag{3.4}$$

$$\int \mathrm{d}\Omega\,\mathrm{d}\Theta = 4\pi \tag{3.5}$$

Then, dividing 4π into n directions equally and giving the kth direction a $\boldsymbol{e}_k$ vector,

$$u_i(\varepsilon) = \frac{1}{2}\frac{q_i^2 e^2}{4\pi\varepsilon}\sum_k^n \frac{1}{n}\frac{1}{L_{ik}} \tag{3.6}$$

Thus, MGB radius of ith atom is

$$L_i = \left(\frac{1}{n}\sum_k^n \frac{1}{L_{ik}}\right)^{-1} \tag{3.7}$$

In MGB equation, this MGB radius is regarded as a distance parameter in the Born term. The parameter for the coulomb repulsion term is obtained by expanding Ohno-Klopman approximation[42,43] in which the MGB radius is adopted in place of van der Waals radius,

$$L_{ij} = \sqrt{R_{ij}^2 + \frac{1}{4}\left(L_i + L_j\right)^2} \tag{3.8}$$

From the above derivation, the expanded MGB equation for any kind of solute molecule is obtained,

$$-\Delta G_{\mathrm{s}}^{\mathrm{MGB}} = \alpha\left(1 - \frac{1}{\varepsilon_{\mathrm{r}}}\right)\sum_i^N \left[q_i^2\frac{1}{L_i} + \sum_{j>i}^N \frac{q_i q_j}{\sqrt{r_{ij}^2 + \frac{1}{4}\left(L_i + L_j\right)^2}}\right] \tag{3.9}$$

$$\alpha = -\frac{e^2}{4\pi\varepsilon_0} \tag{3.10}$$

The perturbation term, F^{MGB} based on this MGB equation is combined with the Fock matrix of MOPAC-PM3 hamiltonian.

$$F^{MGB} = \alpha\left(1 - \frac{1}{\varepsilon_r}\right)\sum_{i}^{N}\left[q_i\frac{1}{L_i} + \sum_{j>i}^{N}\frac{q_j}{\sqrt{r_{ij}^2 + \frac{1}{4}(L_i + L_j)^2}}\right] \tag{3.11}$$

3.3. MOMGB programing

The MGB is included into MOPAC-PM3 program is as follows. Total energy of a molecule in MOPAC is,

$$E_{\text{total}} = E_{\text{el}} + \sum_{i}^{N} \sum_{j<i}^{N} E_{ij}^{\text{core}} \tag{3.12}$$

where E_{el} is total electronic energy, E_{ij}^{core} is ith core-jth core repulsion energy, and N is the number of atoms. The total electronic energy is,

$$E_{\text{el}} = \frac{1}{2} \sum_{\mu} \sum_{\nu} P_{\mu\nu} (H_{\mu\nu}^{\text{PM3}} + F_{\mu\nu}^{\text{PM3}}) \tag{3.13}$$

where $P_{\mu\nu}$ is density matrix, $H_{\mu\nu}^{\text{PM3}}$ is the original core hamiltonian being of a one-electron matrix, $F_{\mu\nu}^{\text{PM3}}$ is the original Fock matrix in PM3 method, and μ and ν are valence atomic orbital indices. Adding the MGB term to Fock matrix,

$$F_{\mu\nu} = F_{\mu\nu}^{\text{PM3}} + F_{\mu\nu}^{\text{MGB}} \tag{3.14}$$

where $F_{\mu\nu}^{\text{MGB}}$ is the perturbation term by a dielectric continuum medium. Using MGB equation, $F_{\mu\nu}^{\text{MGB}}$ is defined by

$$F_{\mu\nu}^{\text{MGB}} = \alpha(1 - \varepsilon_{\text{r}}^{-1}) \sum_{i}^{N} \left[\frac{q_i}{2L_i} + \sum_{j>i}^{N} \frac{q_j}{L_{ij}} \right], \mu \in i. \tag{3.15}$$

During the SCF processes, the contribution of dielectric continuum medium introduced by using, $F_{\mu\nu}^{\text{MGB}}$ varies the calculation parameters such as the density matrix, gradient and so on.

The new total core energy, E_{ij}^{core} is defined as,

$$E_{\text{total}}^{\text{core}} = E^{\text{core,MGB}} + \sum_{i}^{N} \sum_{j}^{N} E_{ij}^{\text{core}} \tag{3.16}$$

where $E^{\text{core,MGB}}$ includes the contribution from the dielectric continuum medium and is

$$E^{\text{core,MGB}} = \alpha\left(1 - \frac{1}{\varepsilon_r}\right)\sum_{i}^{N}\left[q_i^2\frac{1}{L_i} + \sum_{j>i}^{N}\frac{q_i q_j}{\sqrt{r_{ij}^2 + \frac{1}{4}(L_i + L_j)^2}}\right] \qquad (3.17)$$

The MOPAC-PM3 program modified to include MGB equation is called **MOMGB**.

The free energy of solvation depends on standard state and standard free energy change for transfer to a 1 mol·dm^{-1} ideal gaseous molecules to a 1 mol·dm ideal solution at 298 K. MOPAC-PM3 calculation parameters are heats of formation, geometries, ionization potentials, dipole moments, etc. at room temperature, 298K. As a result, calculated values is the data at room temperature by MOMGB if the dielectric constant reqested by MOMGB is that for room temperature. The geometry and energy calculated by MOPAC-PM3 are modified by the vibration or rotation at room temperature, but that of MOMGB must consider the entropy of a solvation system, that is, the motion of solute and solvent molecules must be taken into account. So in practice, calculated energy here is basically not the free energy but the enthalpy.

3.4. MOMGB Keywords

In order to run MOMGB program to calculate a solvation free energy, two new keywords, "`MGB`" and "`ER=`" are required in addition to the MOPAC keywords. "`MGB`" allows MGB equation affect PM3 hamiltonian. The dielectric constant which is used by MGB equation can be defined as "`ER=(the value)`". This keyword can be omitted if the solvent is water, i.e. the default value for the dielectric constant is 78.304.

MOMGB requires MOPAC keyword "`PM3`". List 1 is the input to MOMGB calculate solvation energy of phenanthrene mono-cation in acetonitrile. The keyword "`VECTORS`" is an instruction for dumping out eigen value and eigen vector. The keyword "`CHARGE=1`" indicates +1 charge on solute molecule. The keyword "`T=86400`" limits the total calculation time to 86400 seconds (24 hours). These keywords in MOMGB must be written on a top line in a similar manner as MOPAC.

The second and third lines are used as comment lines. From the forth line the coordinates of atoms of solute molecule are given in the Z-matrix form.

List 1. Input file for MOMGB calculation. The sample is Phenanthrene mono-cation in acetonitrile.

```
PM3 MGB VECT CHARGE=1 ER=35.94 T=86400 XYZ
PHENANTHRENE +1 IN ACETONITRILE
C14H10 +1 IN AN
  C     0.000000  0     0.000000  0     0.000000  0     0     0     0
  C     1.338125  1     0.000000  0     0.000000  0     1     0     0
  C     1.339099  1   118.754303  1     0.000000  0     2     1     0
  C     1.342633  1   120.083107  1     0.000000  1     1     2     3
  C     1.346672  1   120.876617  1     0.000000  1     3     2     1
  C     1.350772  1   122.511864  1     0.000000  1     4     1     2
  C     1.343243  1   118.392952  1   180.000000  1     5     3     2
  C     1.357743  1   124.115715  1   180.000000  1     6     4     1
  C     1.337502  1   120.284103  1   180.000000  1     7     5     3
  C     1.353087  1   119.543839  1   180.000000  1     8     6     4
  C     1.350576  1   124.092278  1     0.000000  1     8     6     4
  C     1.346658  1   121.407219  1   179.999985  1    10     8     6
  C     1.342306  1   122.517632  1   180.000000  1    11     8     6
  C     1.339126  1   120.869064  1     0.000000  1    12    10     8
  H     1.103449  1   119.578369  1   180.000000  1     1     2     3
  H     1.103067  1   120.524605  1   179.999985  1     2     1     3
  H     1.103501  1   117.834312  1   179.999985  1     3     2     1
  H     1.099151  1   114.703850  1   180.000000  1     4     1     2
  H     1.103693  1   121.426720  1     0.000000  1     7     5     3
  H     1.103692  1   118.295670  1   179.999985  1     9     7     5
  H     1.099146  1   122.788696  1     0.000000  1    11     8     6
  H     1.103500  1   121.287888  1   179.999985  1    12    10     8
  H     1.103451  1   120.349586  1   180.000000  1    13    11     8
  H     1.103068  1   120.711113  1   180.000000  1    14    12    10
0
```

3.5. References

[1] M. Born, *Z. Phys.* 1 (1920) 45.

[2] R. Bonaccorsi, R. Cimiraglia, J. Tomasi, *Chem. Phys. Lett.* 99 (1983) 77.

[3] S. Miertus, E. Scrocco, J. Tomasi, *Chem. Phys.* 55 (1981) 117.

[4] S. Miertus, J. Tomasi, *Chem. Phys.* 65 (1982) 239.

[5] J. Tomasi, R. Bonaccorsi, F. J. Olivares del Valle, *J. Mol. Struct. (THEOCHEM)* 234 (1991) 401.

[6] R. Bonaccorsi, P. Palla, J. Tomasi, *J. Am. Chem. Soc.* 106 (1984) 1945.

[7] M. Negre, M. Orozco, F. J. Luque, *Chem. Phys. Lett.* 196 (1992) 27.

[8] F. J. Luque, M. J. Negre, M. Orozco, *J. Phys. Chem.* 97 (1993) 4386.

[9] F. J. Luque, F. Illas, M. Orozco, *J. Comput. Chem.* 11 (1990) 416.

[10] F. J. Luque, M. Orozco, *Chem. Phys. Lett.* 168 (1990) 269.

[11] M. Orozco, F. J. Luque, *J. Mol. Struct. (THEOCHEM)* 254 (1992) 31.

[12] AMPAC ver.2.1: D. A. Liotard, E. F. Healy, J. M. Ruiz, M. J. S. Dewar, QCPE Bull. 10 (1990) 123. (QCPE program 506).

[13] H. Hoshi, M. Sakurai, Y. Inoue, R. Chujo, *J. Chem. Phys.* 87 (1987) 1107.

[14] A. Klamt, G. Schuurmann, *J. Chem. Soc. Perkin Trans. 2* (1993) 799.

[15] L. J. Onsager, *J. Am. Chem. Soc.* 58 (1936) 1436.

[16] MOPAC93: J. J. P. Stewart, Fujitsu Limitted, Tokyo, Japan (1993).

[17] C. J. Cramer, D. G. Truhlar, *J. Am. Chem. Soc.* 113 (1991) 8305.

[18] Y. Kim, D. G. Truhlar, M. M. Kreevoy, *J. Am. Chem. Soc.* 113 (1991) 7837.

[19] S. C. Tucker, D. G. Truhlar, Chem. *Phys. Lett.* 57 (1989) 164.

[20] C. J. Cramer, D. G. Truhlar, Chem. *Phys. Lett.* 198 (1992) 74.

[21] W. C. Still, A. Tempczak, R. C. Hawley, T. Hendrickson, *J. Am. Chem. Soc.* 112 (1990) 6127.

[22] T. Kozaki, K. Morihashi, O. Kikuchi, *J. Am. Chem. Soc.* 111 (1989) 1547.

[23] T. Kozaki, K. Morihashi, O. Kikuchi, *J. Mol. Struct.* 168 (1988) 265.

[24] T. Kozaki, K. Morihashi, O. Kikuchi, *Nippon Kagaku Kaishi* 11 (1986) 1409.

[25] G. J. Hijtink, E. de Boer, P. H. van der Meij, W. P. Weijland, *Rev. Trav. Chim. Pays-Bas* 75 (1956) 487.

[26] O. Chavlet, I. Jano, *C. R. Seances Acad. Sci.* 259 (1964) 1867.

[27] I. Jano, *C. R. Seances Acad. Sci.* 261 (1965) 103.

[28] M.H. Abraham, J. Lizzi, *J. Chem. Soc. Faraday Trans. 1* 74 (1978) 1604.

[29] M.H. Abraham, J. Lizzi, *J. Chem. Soc. Faraday Trans. 1* 74 (1978) 2858.

[30] M.H. Abraham, J. Lizzi, E. Kristof, *Aust. J. Chem.* 35 (1982) 1273.

[31] T. Osakai, S. Himeno, A. Saito, *J. Electroanal. Chem.* 360 (1993) 299.

[32] O. Tapia, Quantam Theory of Chemical Reactions; R. Daudel, A. Pullman, L. Salem., A. Veillard, Eds.; Reidel: Dordrecht, 1980; Vol. II, p25.

[33] R. Constanciel, O. Tapia, *Theor. Chim. Acta* 55 (1980) 77.

[34] W. L. Jorgensen, *J. Phys. Chem.* 90 (1986) 1276.

[35] W. L. Jorgensen, J. Tirado-Rives, *J. Am. Chem. Soc.* 110 (1988) 1657.

[36] M. J. S. Dewar, E. G. Zoebisch, E. F. Healy, J. J. P. Stewart, *J. Am. Chem. Soc.* 107 (1985) 3902.

[37] AMSOL: C. J. Cramer, D. G. Truhlar, (QCPE program 606)

[38] J. J. P. Stewart, *J. Comput. Chem.* 10 (1989) 209.

[40] MOPAC Ver.6.00(QCPE #455, VAX version), J.J.P. Stewart, received as Ver.6.01(JCPE P049) for UNIX-Sun SPARCstation version by Kazuhiro Nishida.

[41] R. C. Bingham, M. J. S. Dewar, D. H. Lo, *J. Am.Chem. Soc*. 97 (1975) 1285.

[42] M. J. S. Dewar, W. Thiel, *J. Am. Chem. Soc.* 99 (1977) 4899.

[43] K. Ohno, *Theor. Chim. Acta* 2 (1964) 219.

[44] G. Klopman, *J. Am. Chem. Soc.* 86 (1964) 4550.

Chapter 4 Applications of the MOMGB.

4.1. The solvation free energies of Polycyclic Aromatic Compounds in Acetonitrile.

4.1.1. Introduction

Solvation free energy is evaluated by MOMGB as follows. The total energy calculated from MOMGB, $E_{\text{total}}^{\text{MGB}}$ is the energy that is required to make up the solute molecule in solvent being continuum medium. It consists of the interaction energy between solute molecule and continuum medium and the formation energy of the solute molecule itself. That is, the solvation free energy $\Delta G_{\text{s}}^{\text{MGB}}$ is,

$$\Delta G_{\text{s}}^{\text{MGB}} = E_{\text{total}}^{\text{MGB}} - E_{\text{total}}^{\text{PM3}}, \qquad \textbf{(4.1)}$$

where $E_{\text{total}}^{\text{PM3}}$ is the total formation energy of the solute molecule in vacuum and obtained from MOPAC-PM3 calculation. The diagram for this process is given in Fig.4.1.1. In MOPAC calculation, PM3 hamiltonian was used. By the use of PM3 (Parametric Method 3) method it is possible to calculate the formation energy and structure of a molecule with considerable chemical accuracy and to estimate the hydration interaction. $E_{\text{total}}^{\text{MGB}}$ is the total formation energy of solute molecule in solvent and obtained from MOMGB calculation. $E_{\text{total}}^{\text{MGB}}$ reflects the energy changes which include the electronic contribution, steric contribution, and solute-solvent interactions. However, these contributions cannot be separated out individually, because they influence each other. For example, the change in charge distribution varies the solute-solvent interaction, which is stood for by MGB equation in MOMGB, and then the succeeding processes of SCF iteration and geometry optimization give rise to new contributions and interactions.

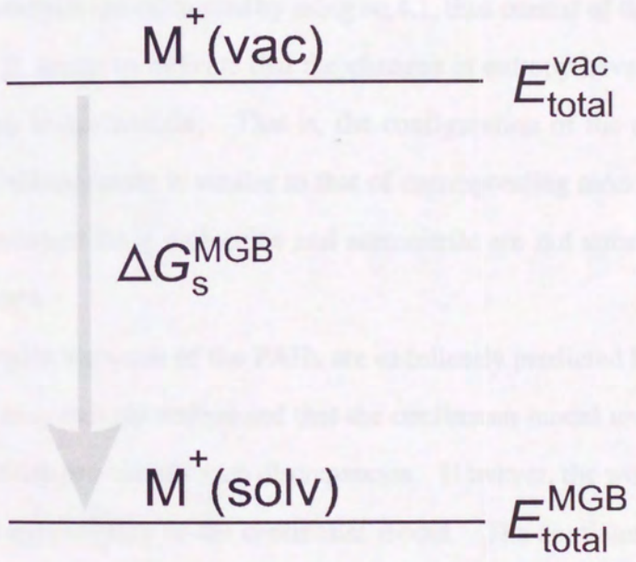

Fig.4.1.1. Schematic dyagram for MOMGB calculation.

4.1.2. Results and Discussion

In Table 4.1.1 are listed the total energies of PAH cations in acetonitrile calculated by MOMGB and those in vacuum by MOPAC and the calculated solvation free energies by eq.(4.1) and experimental ones. Geometries of PAH cations were optimized in vacuum phase and also in acetonitrile. The comparison of the theoretical with the experimental values is given in Fig.4.2. The linear line indicates where the theoretical one is the same as the experimental. The experimental data are of the electrostatic part in the solvation free energies. The calculated values are in fair agreement with experimental ones.

The solvation free energies are calculated by using eq.4.1, thus consist of the enthalpy terms only. The result in Fig.4.1.2. seems to indicate that the changes in entropy have no importance in the system of PAH cations in acetonitrile. That is, the configuration of the acetonitrile molecules surrounding neutral PAH molecule is similar to that of corresponding mono-cation. The solute-solvent interactions between PAH molecules and acetonitrile are not strong enough to vary the entropies in their systems.

The solvation energies for some of the PAHs are excellently predicted by MOMGB, some of about 0.15 eV. One may naively understand that the continuum model used by MOMGB as an approximate method which procedures such discrepancies. However, the worse results seem to be not due to the limited applicability of the continuum model. The continuum model should give larger error for smaller solute ion. In practice, large PAH cations such as perylene and pyrene have the large error(0.15 eV) whereas a small PAH cation such as benzene has the small error(0.04eV). Thus the use of continuum model may not be the main cause for the large errors. These large errors for some molecules are possible to be due to MOPAC calculation itself. MOMGB program is based on MOPAC program. MOPAC is a semi-empirical M.O. calculation program package and its parameters are empirically determined by using a number of experimental data. However, formation energies of some of the PAH molecules are not well predicted by MOPAC calculation many reported [1-7] around 10% errors for the formation energies by AM1 hamiltonian as listed in Table 4.2 PM3 is used in this work. Many suggested in their reports that the parameters for PAH

TABLE 4.1.1. Solvation free energies of PAH cation in acetonitrile from experimental data and calculation using MOMGB and MOPAC-PM3 ($\Delta G_s^{MGB} = E_{total}^{MGB} - E_{total}^{PM3}$).

solute cation	E_{total}^{PM3} /eV	E_{total}^{MGB} /eV	$-\Delta G_s^{MGB}$ /eV	$-\Delta G_s^{expl}$ /eV
benzene	-793.39	-795.35	1.96	1.92
naphthalene	-1298.80	-1300.42	1.62	1.59
anthracene	-1803.70	-1805.10	1.40	1.32
phenanthrene	-1803.57	-1804.99	1.42	1.35
triphenylene	-2308.17	-2309.43	1.26	1.31
pyrene	-2040.85	-2041.46	1.38	1.23
benz[a]anthracene	-2308.31	-2309.58	1.27	1.21
benzo[a]pyrene	-2545.58	-2546.80	1.22	1.22
perylene	-2545.59	-2546.84	1.25	1.10
Benzo[e]pyrene	-2545.74	-2547.01	1.27	1.14
Chysene	-2308.63	-2309.90	1.27	1.22
Benzo[b]triphenylene	-2813.21	-2814.41	1.20	1.16
Benzo[a]chrysene	-2813.31	-2814.50	1.19	1.16
Dibenz[a,h]anthrecene	-2813.27	-2814.45	1.18	1.17
Dibenz[a,j]anthracene	-2813.21	-2814.42	1.21	1.12
Coronene	-3019.88	-3021.06	1.18	1.09
Benzo[b]chrysene	-2813.12	-2814.46	1.30	1.17
Napthacene	-2308.60	-2309.83	1.23	1.18

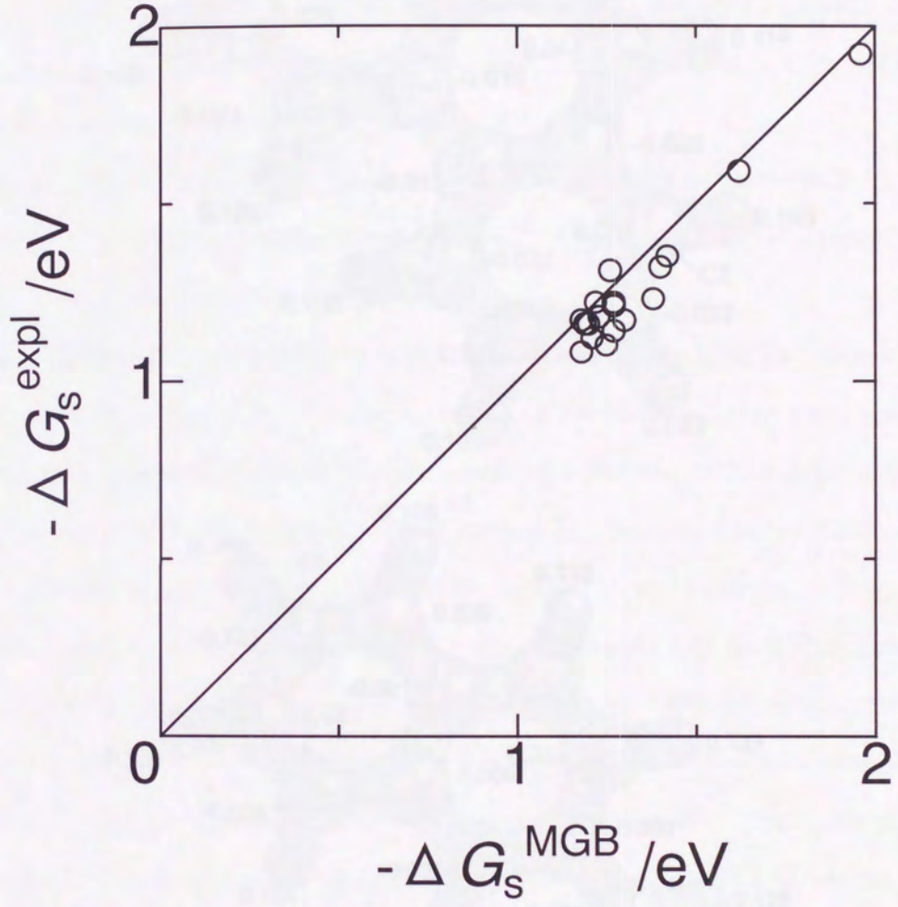

Fig.4.1.2. Correlation of Solvation free energies calculated by MOMGB ΔG_s^{MGB} with experimental ones ΔG_s^{expl} for PAH cations in acetonitrile. The line indicates where $-\Delta G_s^{MGB} = -\Delta G_s^{expl}$.

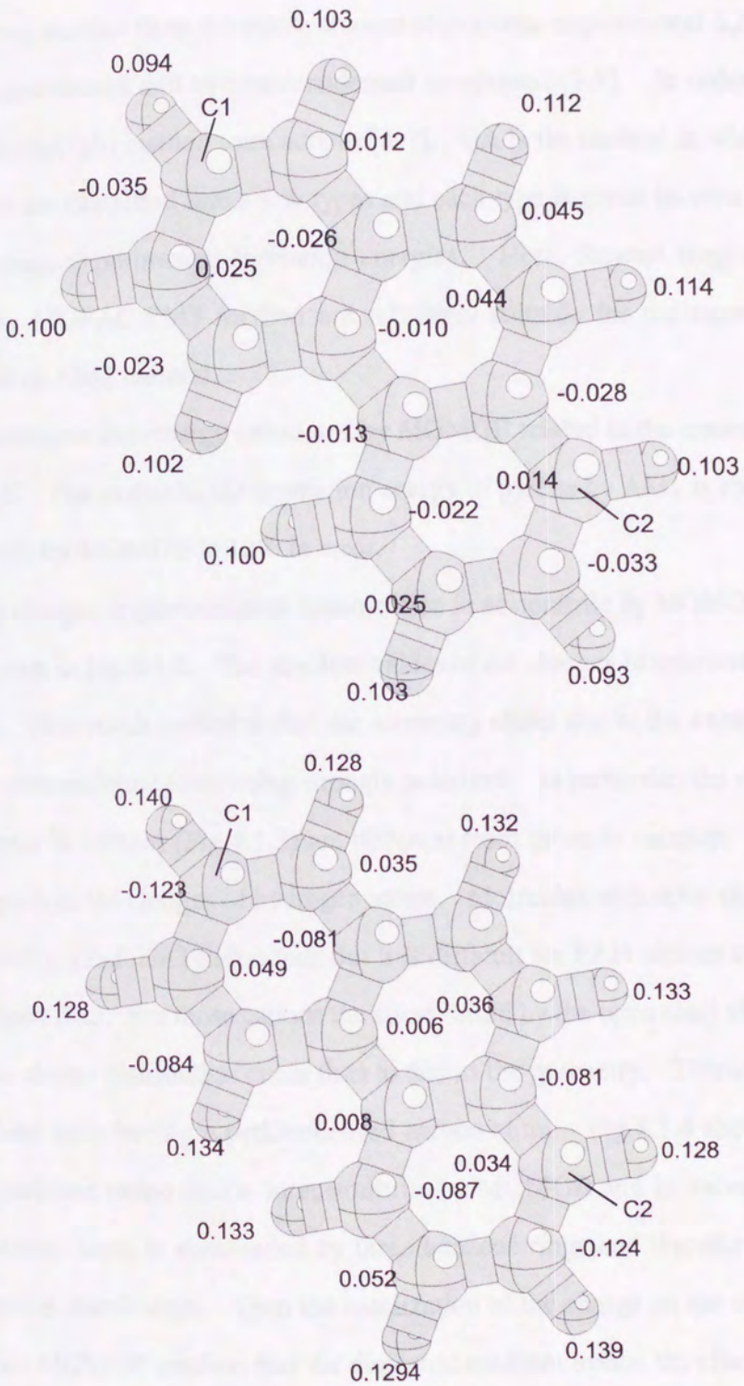

Fig. 4.1.3. Net atomic charges of Phenanthrene in acetonitrile by MOMGB(upper) and in vacuum by MOPAC calculation(lower).

molecules have been derived from the sparse amount of available experimental $\Delta_f H^\circ$ data, i.e. those for only nine catacondensed and two pericondensed compounds[8,9]. In order to correct these errors, group additivity(GA) method were adopted[1-7]. GA is the method in which carbon atoms in PAH molecules are classified into a few types and each type is given its own parameters to be adjusted to reproduce experimental formation energies. Here, Stewart suggested[10] that the calculated data by MOPAC-PM3 method are relatively suitable for the experimental data as comparison to that of AM1 method.

The errors in solvation free energy calculated by MOMGB related to the errors in the formation energy by MOPAC. For example, the formation energy of pyrene by AM1 is about 14% in error. Its solvation energy by MOMGB is 12% in error.

The atomic net charges of phenanthrene mono-cation in acetonitrile by MOMGB and in vacuum by MOPAC are given in Fig.4.1.3. The absolute values of net charges in solovent are smaller than those in vacuum. This result indicates that the screening effect due to the existence of dielectric medium prevents phenanthrene from being strongly polarized. In particular, the atomic net charges of C1 and C2 atoms in solvent (Fig.4.1.3) are different from those in vacuum. Their charges in vacuum nearly equals to the charges of hydrogen atoms. Molecules with open shell structure often deform their geometry, i.e. Jahn-Teller effect, but it is difficult for PAH cations to deform so much because of the steric effect. For those cations the stress raised by the open shell electronic structure tends to distort the charge distribution rather than to distort the geometry. This appears strongly in pyrene and perylene both having a pericondensed carbon atom. Fig.4.1.4 shows the net charge distributions of perylene mono-cation in acetonitrile by MOMGB and in vacuum by MOPAC. Pericondensed carbon atom is surrounded by three benzene rings and therefore keeps tightly its geometry and electric distribution. Then the localization of the charge on the other carbon atoms takes place. While MOMGB predicts that the dielectric medium makes the charge distribution on PAH cation uniform. Therefore, the calculated solvation free energies for pyrene and perylene are over-estimated.

TABLE 4.1.2. Experimental and calculated formation energies(kcal·mol^{-1}) for PAH molecules. AMPAC Austin Model 1 (AM1), Molecular Mechanics 3 (MM3), Molecular Mechanics PC Model (PCM), Group Additivity 1 (GA1), and Group Additivity with Resonance Energy parameter (GARE).

Molecule	expl[a]	AM1[b]	PCM[c]	MM3[c]	GA1[b]	GARE[b]
benzene	20.0	22.0	19.3	20.3	18.4	20.3
naphthalene	36.0	40.6	34.9	36.0	35.8	35.2
anthracene	55.2	62.9	55.6	55.2	53.3	53.8
phenanthrene	49.7	57.4	49.2	50.7	52.2	50.6
benz[a]anthracene	70.3	78.3	68.1	68.6	69.7	67.6
triphenylene	66.5	75.5	66.9	67.5	67.3	67.1
pyrene	54.0	67.4	57.4	58.2	58.6	55.3
perylene	78.4	89.3	79.3	-	73.8	77.2

[a]Pedley, J.B.; Naylor, R.D.; Kirby, S.P., *Thermochemical Data of Organic Compounds*, Chapman and Hall, London, 1986. [b]Herndon, W. C.; Nowak, P. C.; Conner, D. A.; Lin, P. *J.Am.Chem.Soc.* **1992**, *114*, 41. [c]Allinger, N.; Li, F.; Yan, L.; Tai, J., *J.Comput.Chem.* **1990**, *11*, 868.

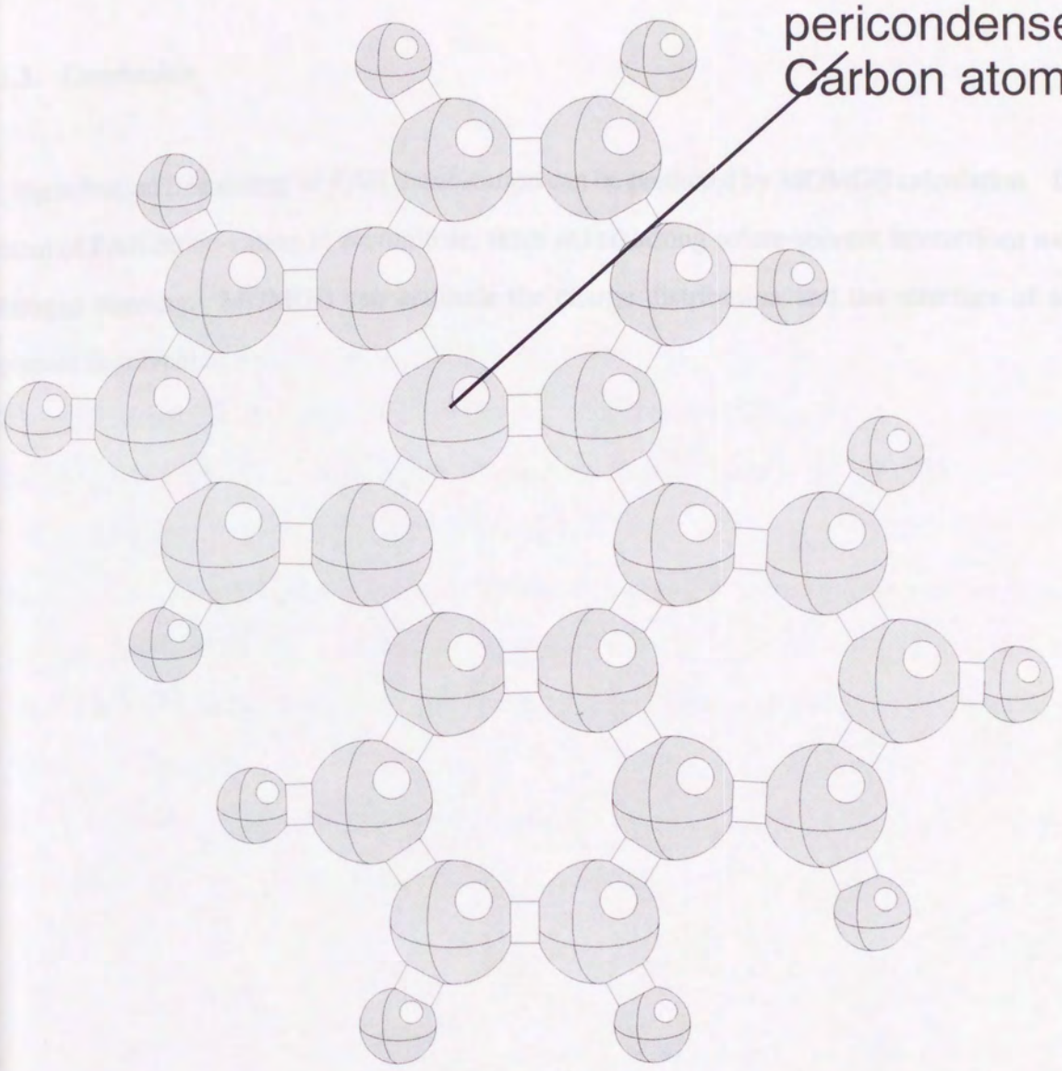
pericondensed
Carbon atom

4.1.3. Conclusion

The solvation free energy of PAH mono-cation can be predicted by MOMGB calculation. In the system of PAH mono-cation in acetonitrile, there are no strong solute-solvent interactions such as hydrogen bonding. MOMGB can estimate the charge distribution and the structure of solute molecule in solvent.

4.1.4. References

[1] S. E. Stein, D. M. Golden, S. W. Benson, *J. Phys. Chem.* 81 (1977) 314.

[2] H. Wang, M. Frenklach, *J. Phys. Chem.* 97 (1993) 3867.

[3] W. C. Herndon, P. C. Nowak, D. A. Conner, P. Lin, *J. Am. Chem. Soc.* 114 (1992) 41.

[4] W. C. Herndon, *J. Am. Chem. Soc.* 112 (1990) 4546.

[5] W. C. Herndon, D. A. Conner, P. Lin, *Pure Appl. Chem.* 62 (1990) 435.

[6] G. R. Somayajulu, B. J. Zwolinski, *J. Chem. Soc., Farad. Trans.* 2 (1974) 1928.

[7] W. C. Herndon, *Israel J. Chem.* 20 (1980) 270.

[8] J. D. Cox, G. Pilcher, Thermochemistry of Organic and Organometallic Compounds; Academic Press: New York, 1970.

[9] J. B. Pedley, R. D. Naylor, S. P. Kirby, Thermochemical Data of Organic Compounds; Chapman and Hall: London, 1986.

[10] J. J. P. Stewart, *J. Comput. Chem.* 10 (1989) 29.

4.2. Calculation of vertical ionization potential of PAH molecules in acetonitrile using MOMGB.

4.2.1. Introduction

One of the solvation parameters is ionization potential of solvated molecule. It can be a measure of its reactivity in a solution, especially when the reaction involves particular or complete electron transfer. The ionization potential in solution have been determined experimentally by photoelectron emission spectroscopy (PEES)[1-3].

In this section, the ionization potentials of PAH molecules in acetonitrile, which were determined by PEES as the photoelectron emission threshold energy, E_t, are estimated by the MOMGB method.

PAH molecule dissolved in acetonitrile, M(solv), can be photoionized by vacuum-ultraviolet light, as follows,

$$M(solv) \rightarrow M^{+*}(solv) + e^{-}(vac) \qquad h\nu_{min} = E_t \tag{4.2.1}$$

where $M^{+*}(solv)$ indicates the exited state of a solute molecule and $h\nu_{min}$ is a lowest required energy for the photoionization of solute molecule, that is, threshold photoionization energy, E_t. The E_t value reflects the energy due to the solute-solvent interaction as well as the ionization potential of the solute molecule in vacuum. There is another one-electron loss process, i.e. the electrochemical oxidation at the electrode. The electrochemistry defines oxidation potential as follows,

$$M(solv) \rightarrow M^{+}(solv) + e^{-}(electrode) \qquad E_{ox}. \tag{4.2.2}$$

It is known that when the electrode is placed at the potential of N.H.E.,

$$e^{-}(electrode) \rightarrow e^{-}(vac) \qquad 4.5\ eV, \tag{4.3.3}$$

then

$$M(solv) \rightarrow M^{+}(solv) + e^{-}(vac) \qquad E_{ox} + 4.5eV. \tag{4.3.4}$$

Both E_t and E_{ox} pertain to the energy for one-electron oxidation of M in solvent. However, they are different in respect of the relaxation of the product M^+ and its surrounding solvent molecules. Thus, $(E_{ox} - E_t)$ value indicates the relaxation energy for the ionization process in solution or the reorganization energy in the Marcus theory[4-8]. The prediction of the E_t value is important when the kinetics of one-electron reaction is discussed.

4.2.2. Theory

The threshold photoionization energy is evaluated by MOMGB as follows. The total energy for M(solv), $E_{total}^{MGB}(\varepsilon_r, q=0)$ is calculated by MOMGB under the condition that the total charge q is zero and the dielectric constant is that of acetonitrile (ε_r=39.4). The total energy for M^{+*}(solv), E (ε, q=1) is calculated by MOMGB under the condition that q = +1 and the dielectric constant is that of optical permittivity for acetonitrile, (ε_{op} = 1.813). The photoionization process in solution is much quicker than the solute-solvent relaxation process (Frank-Condon principle) (Fig.4.2.1). The geometry of the solvents surrounding M^{+*}(solv) does not change during the photoionization process and only the electrons in M^+ relaxes. So the optical permittivity must be used in place of the dielectric constant in the MOMGB calculation. The photoionization threshold energy is obtained as follows (Fig.4.2.2),

$$E_t^{MGB} = E_{total}^{MGB}(\varepsilon_r, q=0) - E_{total}^{MGB}(\varepsilon_{op}, q=1) \tag{4.2.5}$$

The optical permittivity is the square of refractive index, $n^2=(1.346)^2$.

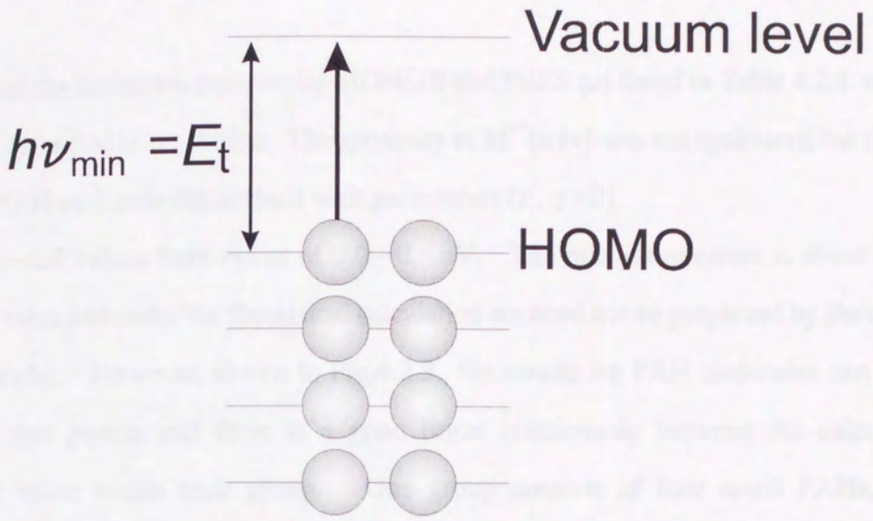

Fig.4.2.1. Schematic Diagram for Photoelectron Emission process.

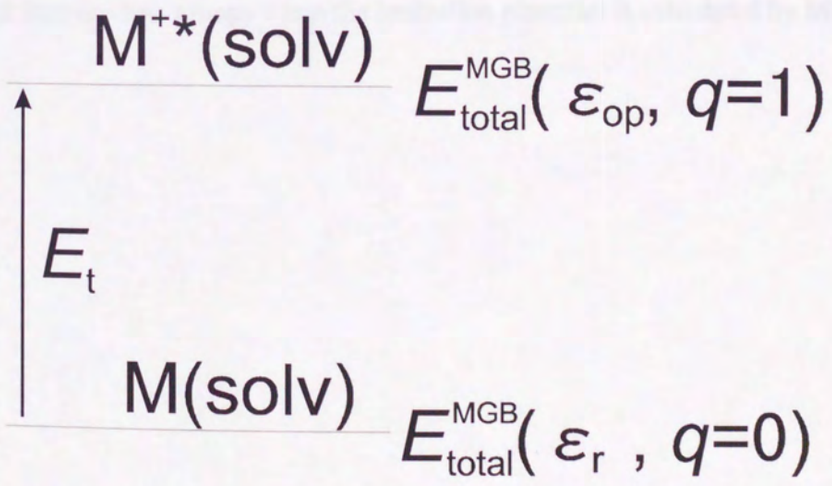

Fig.4.2.2. Diagram for the calculation by MOMGB.

4.2.3. Results and Discussion

The total and the ionization energies by MOMGB and PEES are listed in Table 4.2.1. and plotted in Fig.4.2.3(○) for PAHs in solution. The geometry of M^{+*}(solv) was not optimized but fixed at the geometry of PAH molecule determined with parameters (ε_r, q =0).

The theoretical values have errors of 0.0 - 0.6 eV. The maximum errors is about 8% of the experimental value and under the theoretical calculation we need not be perplexed by the calculation error in this order. However, shown in Fig.4.2.3., the results for PAH molecules can be clearly divided into two groups and there is a good linear relationship between the calculated and experimental value within each group. One group consists of four small PAHs, benzene, naphthalene, anthracene and phenanthrene and another group is composed of five large PAHs, triphenylene, pyrene, benz[a]anthracene, benzo[a]pyrene and perylene. What causes PAH molecules in acetonitrile this classification cannot be clarificated obviously. If we did suggest this reason, the ionization potential depends on how the radical solute PAH molecule interacts with the near solvent acetonitrile in the photoionization process and thus to use a single optical permittivity for both groups happens two groups when the ionization potential is calculated by MOMGB.

TABLE 4.2.1. Experimental and MOMGB Vertical ionization potentials for PAH mono-cations. (Dielectric constant ε_r=35.94, Optical permittivity $\varepsilon_{op}=n^2=(1.346)^2=1.813$)

solute cation	E_{total}^{MGB} (ε_r,q=0) /eV	E_{total}^{MGB} (ε_{op},q=1) /eV	E_t^{MGB} /eV	E_t^{expl} /eV
benzene	-802.73	-794.25	8.48	8.04
naphthalene	-1307.21	-1299.52	7.69	7.04
anthracene	-1811.52	-1804.40	7.12	6.46
phenanthrene	-1811.81	-1804.25	7.56	6.97
triphenylene	-2316.45	-2308.82	7.63	7.46
pyrene	-2048.73	-2041.58	7.15	7.17
benz[a]anthracene	-2316.18	-2308.99	7.19	7.31
benzo[a]pyrene	-2553.18	-2546.26	6.92	6.96
perylene	-2553.16	-2546.30	6.86	6.87

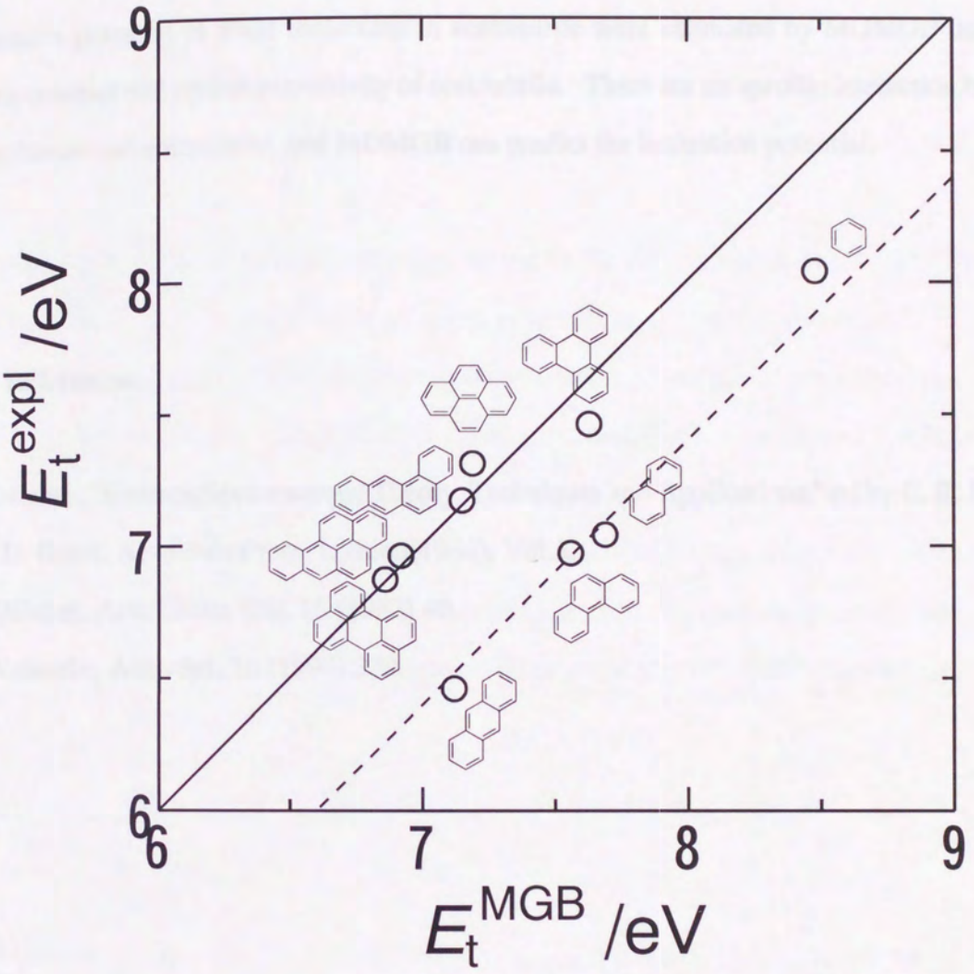

Fig. 4.2.3. Correlation of the ionization potentials in acetonitrile calculated by MOMGB with experimental ones for PAH cations.

4.2.4. Conclusion

Ionization potential of PAH molecules in acetonitrile were estimated by MOMGB using the dielectric constant and optical permittivity of acetonitrile. There are no specific interaction between PAH molecule and acetonitrile, and MOMGB can predict the ionization potential.

4.2.5. References

[1] P. Delahay, "Electron Spectroscopy: Theory, Techniques and Applications," ed by C. R. Brundle and A. D. Baker, Academic Press, London(1984), Vol.5.

[2] P. Delahay, Acc. Chem. Res. 15 (1982) 40.

[3] I. Watanabe, Anal. Sci. 10 (1994) 329.

4.3. Calculation of ionization potentials of Alkoxide anions in water and alcohols using MOMGB.

4.3.1. Introduction

Alkoxide anion is deprotonated and forms strong hydrogen bonding with solvent. Alkoxide anion dissolved in protic solvent such as water or alcohols is strongly coordinated by solvent molecules. Recently, Sakai et al.[1] reported the ionization potentials of alkoxide anions CH_3O^- (MeO^-), $C_2H_5O^-$ (EtO), C H O (PrO), C H O (BuO), including OH , in water and alcohols. They found that although the ionization potentials for a series of alkoxide anions are almost constant each other, 1.6-1.8 eV, in vacuum, they are not in water and alcohols. Thus, the solvent effect must be strongly working on the ionization potential of alkoxide and on their reactivity in solvents. In this chapter, the solvent effect on the ionization potential is treated by MOMGB calculation.

4.3.2. Theory

During the M.O. calculation for alkoxide neutral radicals, it was not possible to achieve the SCF field. Thus, the ionization potential could not be estimated from the total energy difference. Then, instead of calculating the total energies which is the method used for PAH samples, HOMO eigen value was used to predict ionization potential according to the Koopmans' theorem. Koopmans' theorem tells that the eigen value of each orbital with the opposite sign to the original corresponds to the ionization potential for the Hartree-Fock molecular orbital of self-consistent field. This theorem ignores the electron correlation energy and the electron reorganization energy after the ionization process. However, since these effects counteract each other it is fairly good approximation. The case where the Koopmans' theorem breaks down is the system in which the orbital is degenerate. It is because the geometry of molecule and charge distribution vary

significantly by losing the degenerate electron. For example, benzene has C_{3h} symmetry and its HOMO and second HOMO are degenerate. The delocalized HOMO spreads out over 6 carbon atoms of benzene ring.

The process that alkoxide anion is ionized in solvent is,

$$X^-(solv) \rightarrow X^{0*}(solv) + e^-(vac) \qquad \textbf{(4.3.1)}$$

then the product molecule X^{0*} has no charge, while the process that PAH molecule is ionized in solvent is,

$$M(solv) \rightarrow M^{+*}(solv) + e^-(vac) \qquad \textbf{(4.3.2)}$$

then the charge of the product cation M^{+*} is +1. Thus, M interacts the dielectric continuum medium strongly and the final state of M^{+*} is varied compared with the state predicted by Koopmans' theorem. In practice, ionization potential in solvent is smaller than that predicted by Koopmans' theorem.

For example, the eigen value of HOMO for benzene in acetonitrile by MOMGB is 9.98 eV and this value is much larger than the experimental value (8.06 eV). For alkoxide anion, the HOMO is localized on oxygen atom and it is thought that alkoxide anion are satisfied with Koopmans' theorem. Then HOMO eigen value of alkoxide anion, ε_{HOMO}, is calculated by MOMGB.

4.3.3. Results and discussion

The MOMGB calculation results are listed in Table 4.3.1. and plotted in Fig.4.3.1. The agreement between calculated and experimental ionization potentials of a series of alkoxide anions in water is not acceptable, as shown in Fig.4.3.1(□). This is possibly caused by the simple continuum medium model used by MOMGB program. In the MOMGB program, the dielectric constant for the medium is considered to be the same everywhere. However, when the strong interaction such as hydrogen bonding exists between solute and solvent, some solvent molecules specifically coordinate to a solute molecule and their properties must be different from that of the bulk solvent molecules. The dielectric constant used here represents the property of the bulk.

TABLE 4.3.1. Eigen values of HOMO, ε_{HOMO}^{MGB} for alkoxide anion in water coordinated by water determined by MOMGB.

molecules	$-\varepsilon_{HOMO}^{MGB}$ /eV	E_t /eV[a]
OH^-	6.91	8.26
$OH^-(H_2O)$	6.95	
$OH^-(H_2O)_2$	7.61	
$OH^-(H_2O)_3$	7.96	
$OH^-(H_2O)_4$	8.00	
$OH^-(H_2O)_{13}$	8.07	
MeO^-	6.93	7.67
$MeO^-(H_2O)$	7.11	
$MeO^-(H_2O)_2$	7.42	
$MeO^-(H_2O)_3$	7.66	
EtO^-	6.70	7.58
$EtO^-(H_2O)$	6.88	
$EtO^-(H_2O)_2$	7.22	
$EtO^-(H_2O)_3$	7.55	
PrO^-	6.71	7.56
$PrO^-(H_2O)$	6.87	
$PrO^-(H_2O)_2$	7.26	
$PrO^-(H_2O)_3$	7.53	
BrO^-	6.71	7.47
$BrO^-(H_2O)$	6.90	
$BrO^-(H_2O)_2$	7.24	
$BrO^-(H_2O)_3$	7.54	
$BrO^-(H_2O)_4$	7.57	

[a]Reference 1,4.

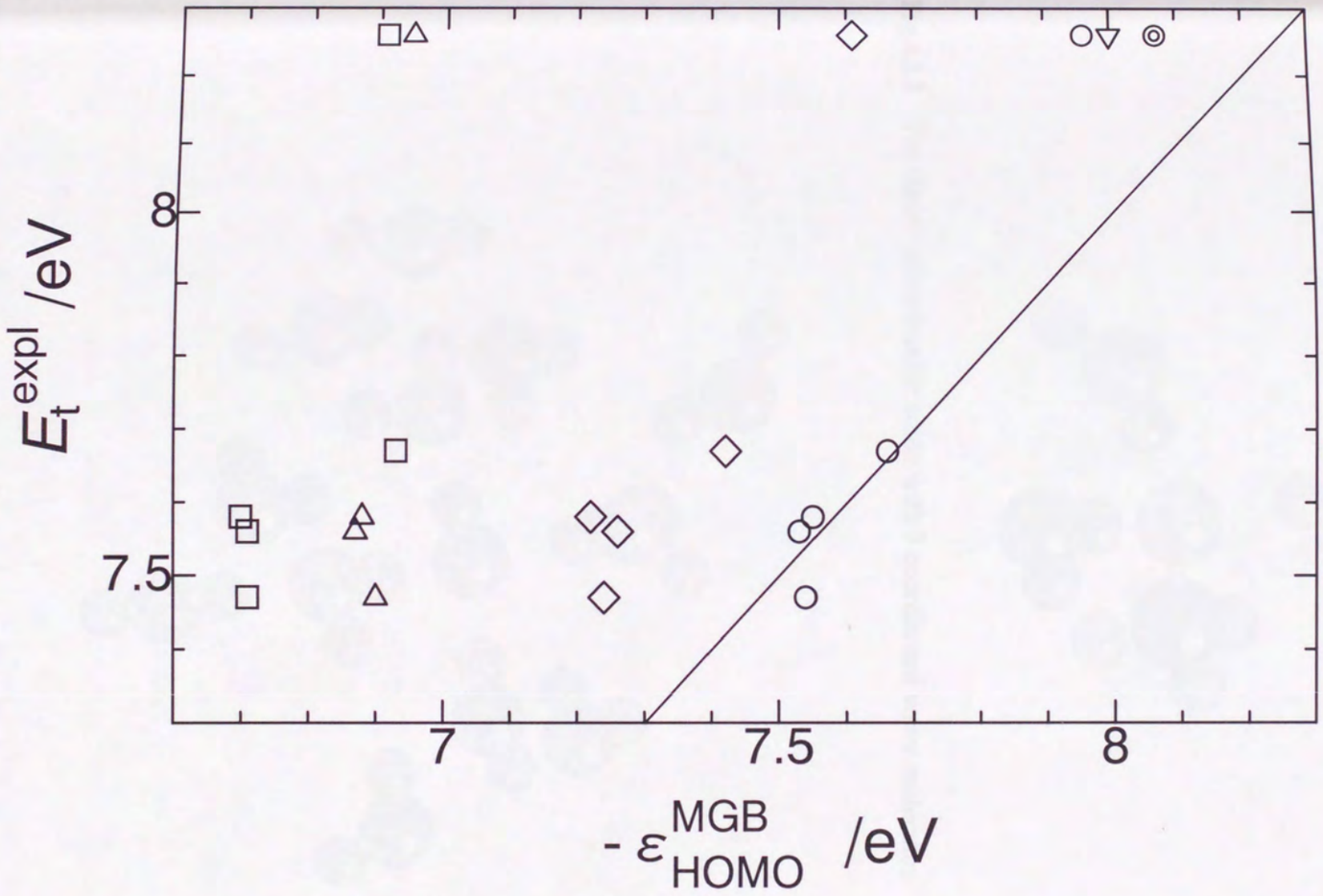

Fig. 4.3.1. Correlation of $-\varepsilon_{HOMO}^{MGB}$ calculated by MOMGB with E_t values for alkoxide anion in water. The number of coordinated water; 0 (□), 1(△), 2(◇), 3(○), 4(▽), 13(◎).

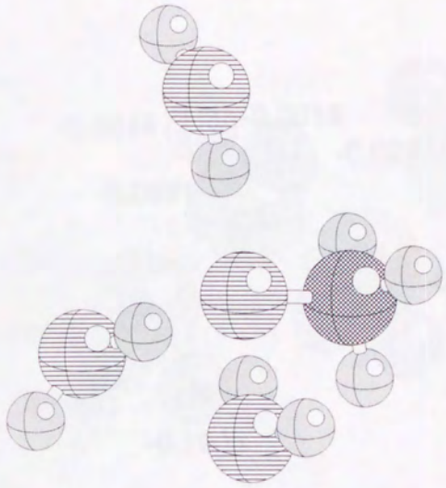

Fig.4.3.2. The cluster of methoxide anion with 3 coordinated water molecules.

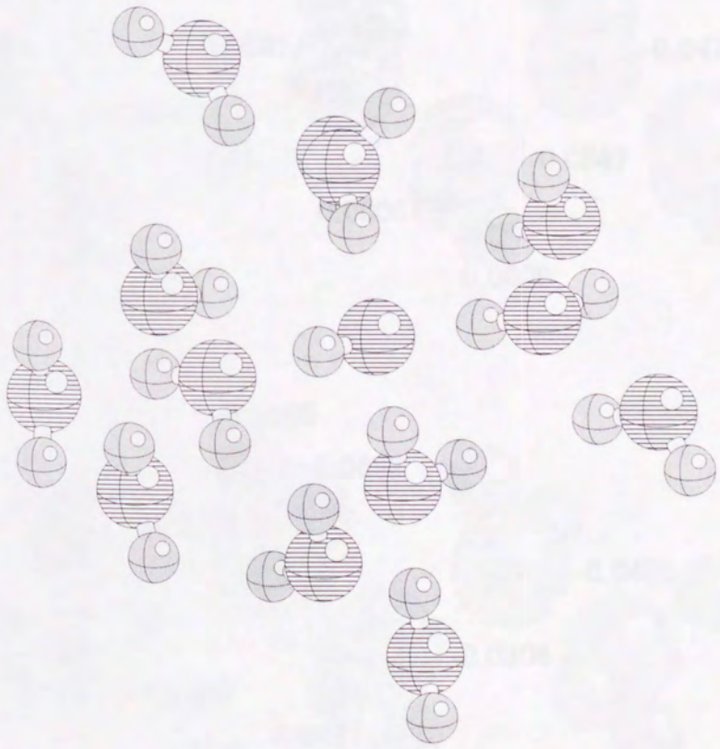

Fig.4.3.3. The cluster of hydroxide anion with 13 coordinated water molecules.

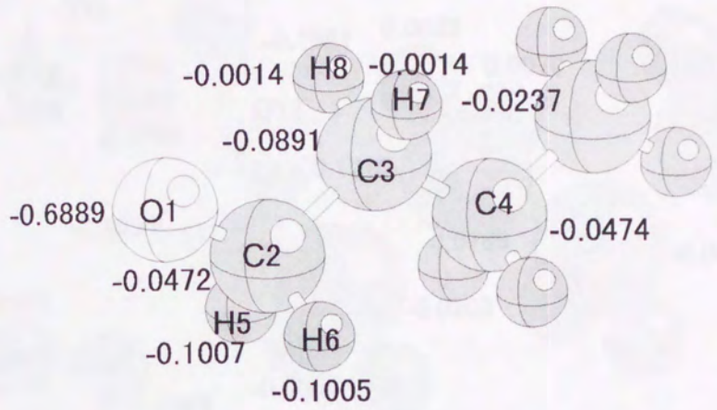
-0.0014
H8
-0.0014
H7
-0.0237
-0.0891
C3
C4
-0.6889
O1
-0.0474
C2
-0.0472
H5
H6
-0.1007
-0.1005

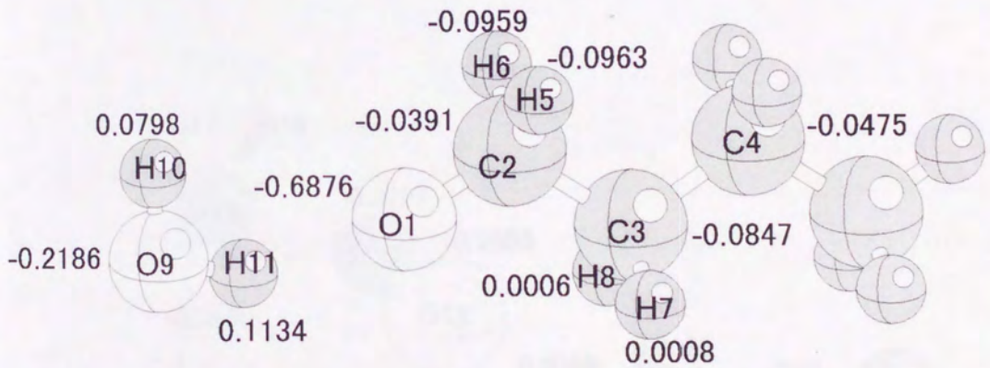
-0.0959
H6
-0.0963
H5
0.0798
-0.0391
C4
-0.0475
H10
C2
-0.6876
O1
C3
-0.0847
-0.2186
O9
H11
0.0006
H8
H7
0.1134
0.0008

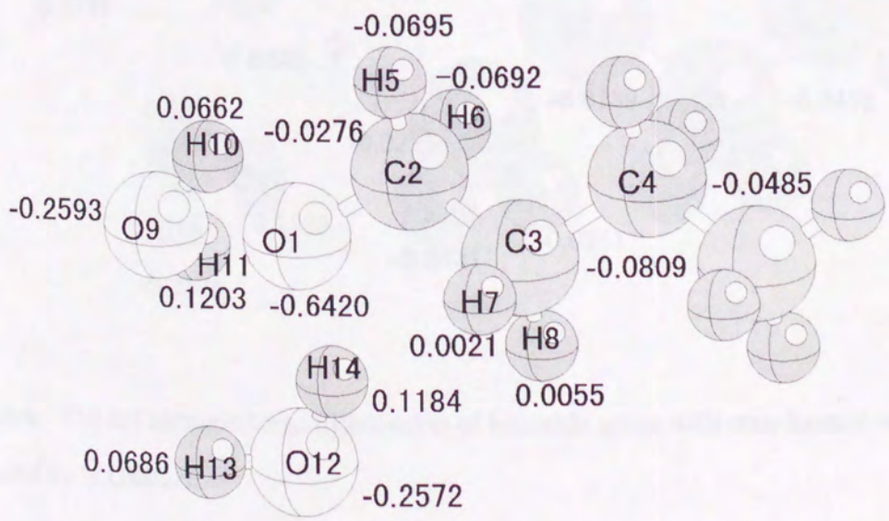
-0.0695
H5
−0.0692
0.0662
H6
H10
-0.0276
C2
C4
-0.0485
-0.2593
O9
O1
C3
H11
-0.0809
0.1203
-0.6420
H7
0.0021
H8
H14
0.1184
0.0055
0.0686
H13
O12
-0.2572

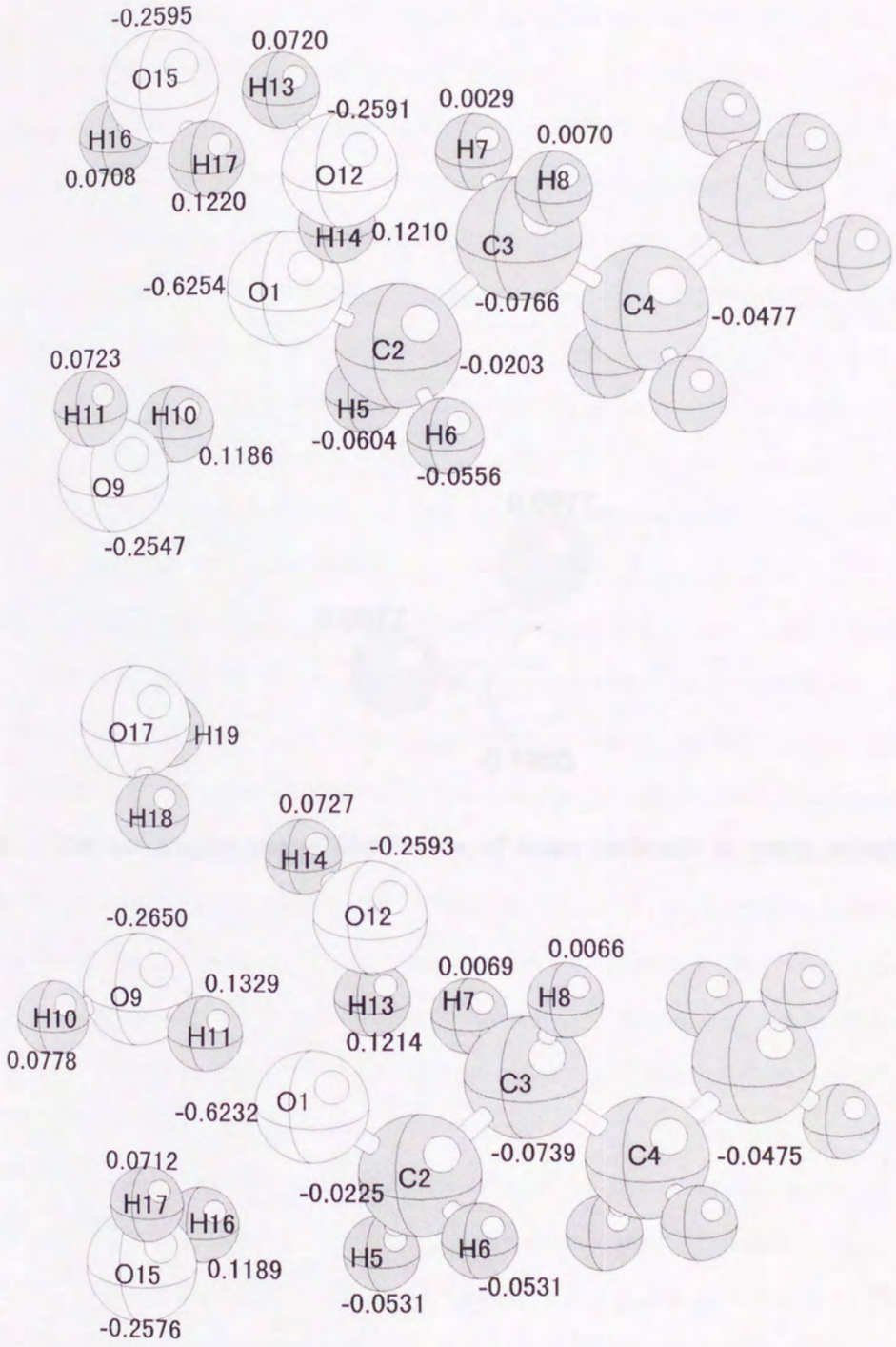

Fig. 4.3.4. The net atomic charge distribution of butoxide anion with coordinated water molecules calculated by MOMGB.

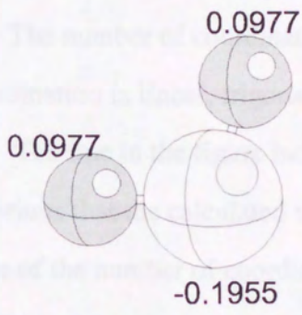

Fig. 4.3.5. The net atomic charge distribution of water molecule in water calculated by MOMGB.

Thus, in the system for which the experimental values can be predicted by using the dielectric continuum model such as the PAH mono-cation in acetonitrile, the character of solvent molecules surrounding a solute molecule must be almost the same as that of the bulk. On the other hand, in the system like alkoxide anion in water, it seems that the experimental values could not be reproduced by the dielectric continuum model in order to include the specific solute-solvent interactions like hydrogen bonding and thus their specific interaction must be taken into account. Then, a cluster model is built up by coordinating some water molecules to the oxygen atom of alkoxide anion. Fig.4.3.2 shows the cluster of methoxide anion with three coordinated water molecules. The MOMGB calculation is carried out using this cluster and the results are listed in Table 4.3.1 and plotted in Fig.4.3.1. The number of coordinated water molecules is 1(△), 2(◇) or 3(○) and the geometry of the coordination is linear, trigonal-planar, or tetrahedral for oxygen atom of alkoxide anion, respectively. The line in the figure indicates where the theoretical one is the same as the experimental. It is obvious that the calculated values are in better agreement with the experimental ones with the increase of the number of coordinated water molecules. However, as shown for a butoxide anion case in Table 4.3.1, the result of the MOMGB calculation seems not to be improved further by adding more than four water molecules. The charge distribution in the cluster having four coordinated water molecules is also similar to that having three coordinated water molecules. There is little effect of the existence of more than four water molecule's on HOMO level. That is, it seems that the number of water molecule interacting with the oxygen atom of butoxide anion in water is 3 in MOMGB calculation. The net charge distributions for butoxide anion with 0, 1, 2, 3 and 4 coordinated water molecules are illustrated in Fig.4.3.4. The charge on the oxygen atom of the butoxide anion (O1 denoted in Fig.4.3.4) decreases as the number of coordinated water molecule increases. The charge on C4 atom is almost constant. The change of the charge of O1 atom in butoxide anion hardly influences the charge of C4 atom. Thus, this predicts that the charge of O1 atom will be about the same if the length of $-CH_2-$ chain away from C4 atom should vary. The charge distribution of the coordinated water molecules is fairly different from the bulk water molecule calculated by MOMGB shown in Fig.4.3.5 and it is suggested that their water molecules cannot be approximated by the dielectric continuum medium with the same

TABLE 4.3.2. Eigen values of HOMO, ε_{HOMO}^{MGB} for alkoxide anion in alcohols coordinated by water determined by MOMGB.

molecules	solvent	$-\varepsilon_{HOMO}^{MGB}$ /eV	E_t /eV[a]
OH^-	H_2O	6.91	8.26
$OH^-(H_2O)$		6.95	
$OH^-(H_2O)_2$		7.61	
$OH^-(H_2O)_3$		7.96	
$OH^-(H_2O)_4$		8.00	
$OH^-(H_2O)_{13}$		8.07	
MeO^-	MeOH	6.48	7.53
$MeO^-(MeOH)$		6.55	
$MeO^-(MeOH)_2$		6.96	
$MeO^-(MeOH)_3$		7.30	
EtO^-	EtOH	6.27	7.34
$EtO^-(EtOH)$		6.38	
$EtO^-(EtOH)_2$		6.79	
$EtO^-(EtOH)_3$		7.18	
PrO^-	PrOH	6.20	7.13
$PrO^-(PrOH)$		6.34	
$PrO^-(PrOH)_2$		6.65	
$PrO^-(PrOH)_3$		7.14	
BrO^-	BuOH	6.20	6.96
$BrO^-(BrOH)$		6.30	
$BrO^-(BrOH)_2$		6.65	
$BrO^-(BrOH)_3$		7.07	

[a]Reference 4.

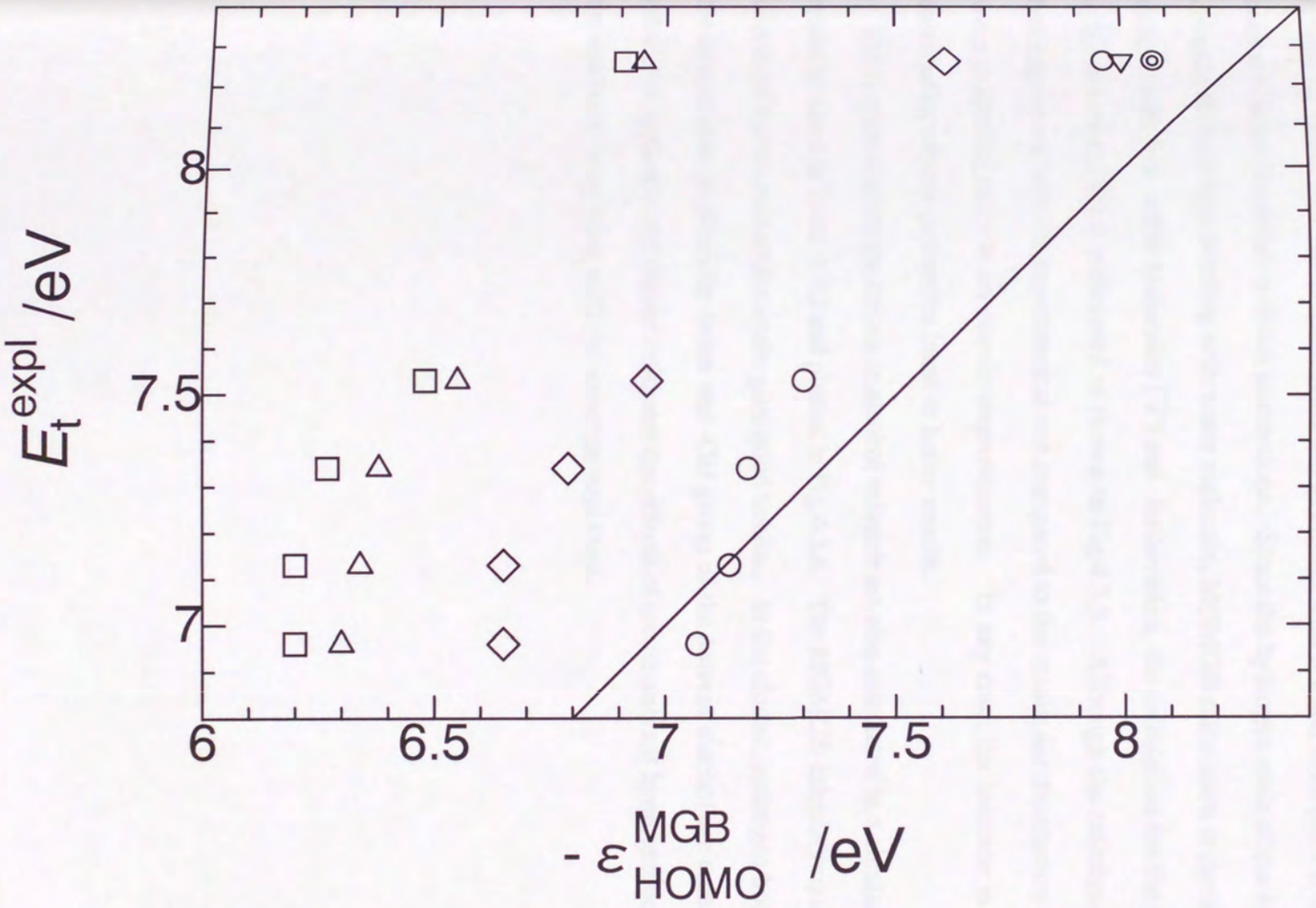

Fig. 4.3.6. Correlation of $-\varepsilon_{HOMO}^{MGB}$ calculated by MOMGB with E_t values for alkoxide anion in alcohols. The number of coordinated water; 0(□), 1(△), 2(◇), 3(○), 4(▽), 13(◎).

property as the bulk molecule. Since MOPAC-PM3 method used by MOMGB can estimate the contribution of the hydrogen bonding by introducing the specific parameters for O···H and N···H bonding, the use of the cluster model leads to better agreement with the experimental values.

The error for calculated value of a hydroxide anion is larger than those of the other alkoxide anions. It seems that this is becausethe use of cluster with 3 water molecules is not sufficient in order to estimate the solute-solvent interactions. Since the hydrogen atom of the hydroxide anion can make the hydrogen bonding with water molecule, MOMGB calculation is carried out by using a cluster with four water molecules (▽) and furthermore, the calculation for the cluster with 13 water molecules (◎) is performed as shown in Fig.4.3.3. Although the calculated values are in better agreement with the experimental one compared to the results for the clusters with 1, 2 and 3 water molecules, there is no drastic improvements. In any case, the increase in the number of coordinating solvent molecules lease to better results.

The systems of alkoxide anions in alcohol solvents are also calculated in a similar manner. The results are listed in Table 4.3.2 and plotted in Fig.4.3.6. The MOMGB calculations using the cluster with three solvent molecules again give good results. In the cluster, hydrogen bondings between the oxygen atom of alkoxide anion and -OH group of the solvent alcohol are created. MOMGB calculation applied to the cluster estimates the effects of solute-solvent hydrogen bonding well and the results are compatible with the experimental ones.

4.3.4. Conclusion

Ionization potentials of anions in solvent were estimated from the eigen value of HOMO in MOMGB calculation under he approximation of Koopmans' theorem.

MOMGB calculation has no specific parameters to include hydrogen bonding effects and thus there are large errors in the calculated values under the existence of the specific interaction. In order to take into account the specific interaction, the cluster model having some solvent molecules is used in MOMGB calculation. Then, their interactions is estimated by MOPAC-PM3 method. The calculated values by MOMGB using the cluster model are in agreement with the experimental ones.

4.3.5. References

[1] K. Sakai, I. Watanabe, Y. Yokoyama, Bull. Chem. Soc. Jpn. 67 (1994) 360.

[2] Koopmans, Physica, 1 (1933) 104.

[3] E. Mentasti, E. Pelizzetti, E. Pramaudo, J. Inorg. Nucl. Chem. 37 (1975) 1733.

[4] K. Sakai, Master's thesis, Osaka University, Osaka, Japan, 1994.

4.4. Calculation of Solvation free energies and Ionization Potentials of Bromide Anions in Various Solvents.

4.4.1. Introduction

The previous sections discribe the calculations of solvation energies and ionization potentials of PAH mono-cations in acetonitrile and alkoxide anions in water or alcohols by using MOMGB and MOPAC.

Tanida et al. reported ionization potentials determined by PEES[1-5] of a bromide anion in various solvents and the distance between bromide anion and the nearest or second nearest atom of the coordinated solvent by EXAFS (extended X-ray absorption fine structure) method[1,6-8].

In this section, the calculation of the solvation energies and ionization potentials of the bromide anion in various solvents are carried out. Solvents used in the MOMGB calculation in this section are water (H_2O), methyl alcohol (MeOH), ethyl alcohol (EtOH), propyl alvohol (PrOH), pyridine (Py), nitromethane (NM), and *N*-methyl-2-pyrolidinone (NMP). The differences of solvation energy and ionization potential among the solvents are predicted by MOMGB calculation with cluster model.

4.4.2. Theory

In the scssion 4.3, the ionization potentials of alkoxide anions in water or alcohols are calculated by using MOMGB method with the cluster models which include alkoxide anion and some water or alcohol molecules. Modeling the cluster is a powerful means in order to take into account the specific solute-solvent interaction. The calculation of solvation energies are run by using the cluster model in MOMGB. The total energy of the cluster calculated by MOMGB includes the formation energies of solute and solvent molecules and the solvation energy depending on the solute-solvent

interactions. That is, the solvation enegry is defined as follows,

$$\Delta G_s^{MGB} = E_{total}^{MGB}(\text{cluster}) - (E_{total}^{PM3}(Br^-) + N \cdot E_{total}^{PM3}(\text{solvent})) \qquad \textbf{(4.4.1)}$$

where N is the number of solvent in the cluster.

4.4.3. Results and Discussion

Solvation free energies.

The total energies and the solvation energies calculated by MOMGB for bromide anion in various solvents are listed in Table 4.4.1 along with the experimentally observed solvation energies and plotted in Fig.4.4.1. These values were calculated for one bromide anion embedded in a dielectric medium with the dielectric constant ε_r. It is reasonable that the results corresponds to ε, since these results are derived from the crassical Born equation. The solute-solvent interaction is considered with only ε_r in this case. Then, when the solute-solvent interaction of one system resembles that of another system, the calculated value by using only dielectric constant (the treatment of classical Born equation) corresponds to the experimental one. It is thought that these solvents can solvate with bromide anion through the interaction of the hydrogen atom of -OH functional group. The interaction between the bromide anion and the hydrogen atom of -OH group is not a specific interaction such as O···H hygrogen bonding but mainly a simple electrostatic interaction. That is, the trend of the solvation free energies among these solvents is predicted by MOMGB without postulating the cluster. However, the solvents such as NM, Py, and NMP may interact with the bromide anion with the different mannar from the protic solvents.

TABLE 4.4.1. Calculation of Solvation free energies of Bromide anion in various solvents.

Solvent	ε_r	E_{total}^{MGB} /eV	$-\Delta G_s^{MGB}$ /eV	$-\Delta G_s^{expl}$ /eV[a]
H_2O	78.30	-357.99	1.85	3.14
MeOH	32.66	-357.96	1.82	3.02
EtOH	24.55	-357.94	1.80	2.95
PrOH	20.45	-357.92	1.78	2.91
NM	35.87	-357.96	1.82	2.84
Py	12.91	-357.87	1.73	2.92
NMP	32.20	-357.95	1.81	2.76

$\Delta G_s^{MGB} = E_{total}^{MGB} - E_{total}^{PM3}(Br^-)$. $E_{total}^{PM3}(Br^-)$=-356.14eV.

[a] P. Delahay, A. Dziedzic, *Proc. Indian Acad. Sci.* 97 (1986) 221.; T. M. Miller, B Bederson, *Adv. At. Mol. Phys.* 13 (1977) 1.; J. D. Lamb, J. J. Christensen, S. R. Izatt, K. Bedke, M. S. Astin, R. M. Izatt, *J. Am. Chem. Soc.* 102 (1980) 3399.

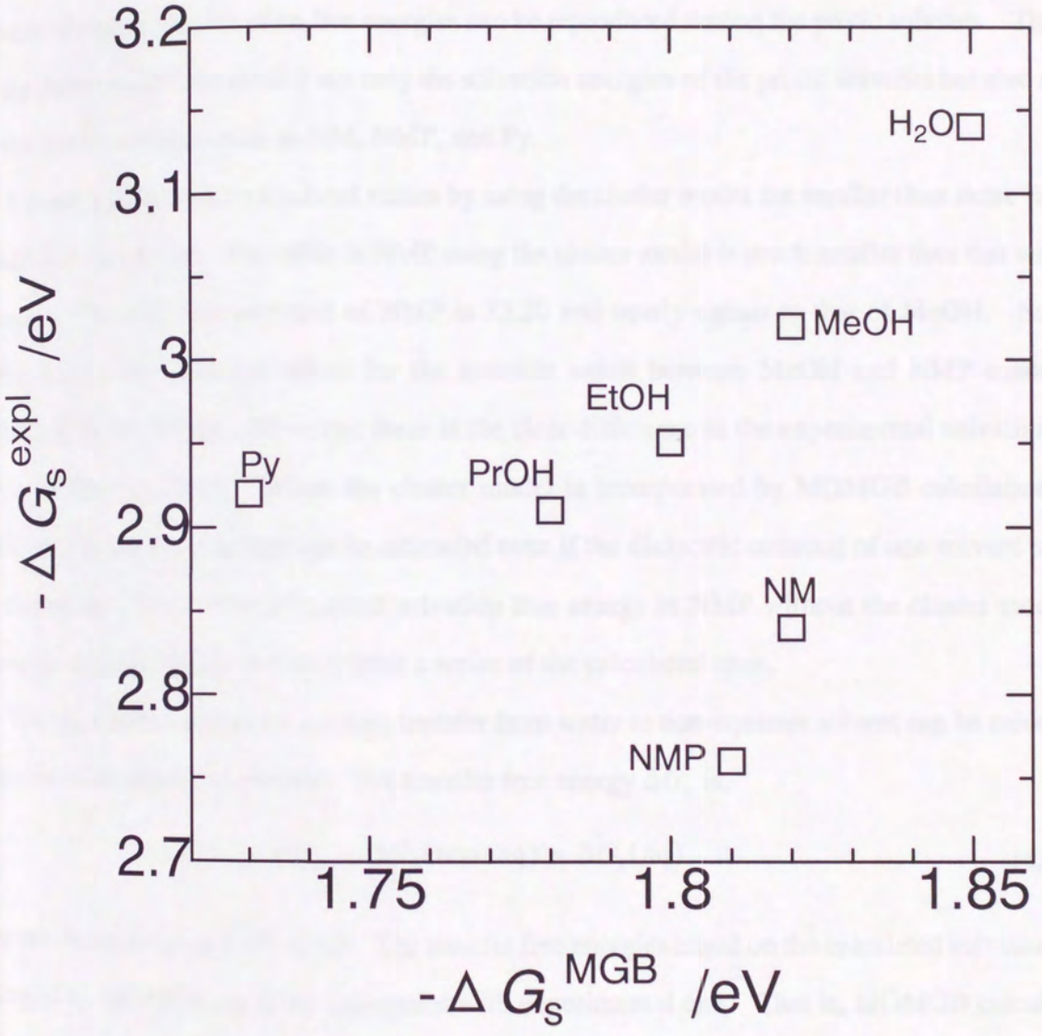

Fig. 4.4.1. Correlation of the solvation energy calculated by MOMGB with the experimental one for bromide anion in various solvents.

The calculated values by MOMGB using the cluster are listed in Table 4.4.2 and plotted in Fig4.4.2(○). The cluster models for the solvation of bromide anion are shown in Fig.4.4.3. From Fig.4.4.2., the calculated value by MOMGB using the cluster clearly corresponds to the experimental one. In the case of caluclation for only bromide anionwith no application of the cluster model, the relative change in the solvation free energies can be reproduced among the protic solvents. The use of the cluster model can predict not only the solvation energies of the protic solvents but also those of the aprotic solvents such as NM, NMP, and Py.

It is noticed that some calculated values by using the cluster model are smaller than those for the model without cluster. The value in NMP using the cluster model is much smaller than that without cluster. The dielectric constant of NMP is 32.20 and nearly equals to that of MeOH. So, the difference of the solvation effect for the bromide anion between MeOH and NMP cannot be estimated by MOMGB. However, there is the clear difference in the experimental solvation free energies between them. When the cluster model is incorporated by MOMGB calculation, the difference in solvation energy can be estimated even if the dielectric constant of one solvent equals to that of the other. The calculated solvation free energy in NMP without the cluster model of bromide anion is largely deviated from a series of the calculated ones.

The transfer free energy for a solute transfer from water to non-aqueous solvent can be calculated from each solvation free energy. The transfer free energy ΔG_{tr} is,

$$\Delta G_{tr} = \Delta G_s(\text{non-aq}) - \Delta G_s(\text{aq}) . \qquad \textbf{(4.4.2)}$$

The results are listed in Table 4.4.3. The transfer free energies based on the calculated solvation free energies by MOMGB are fairly agreement with experimental one. That is, MOMGB calculation can be used for the prediction of the transfer free energy in various solvents with respect to each other.

TABLE 4.4.2. Calculation of Solvation free energies of Bromide anion in various solvents.

Solvent	N	E_{total}^{MGB} (cluster) /eV	E_{total}^{PM3} (solvent) /eV	$-\Delta G_s^{MGB}$ /eV	$-\Delta G_s^{expl}$ /eV
H_2O	6	-2307.09	-324.91	1.95	3.14
MeOH	4	-2254.61	-474.15	1.87	3.02
EtOH	4	-2852.52	-623.67	1.70	2.95
PrOH	4	-3450.60	-773.20	1.66	2.91
NM	4	-2832.90	-618.77	1.68	2.84
Py	4	-3682.12	-831.06	1.74	2.92
NMP	4	-5109.00	-1187.85	1.46	2.76

$\Delta G_s^{MGB} = E_{total}^{MGB} - (E_{total}^{PM3} (Br^-) + N \cdot E_{total}^{PM3} (solvent))$. $E_{total}^{PM3} (Br^-)$=-356.14eV.

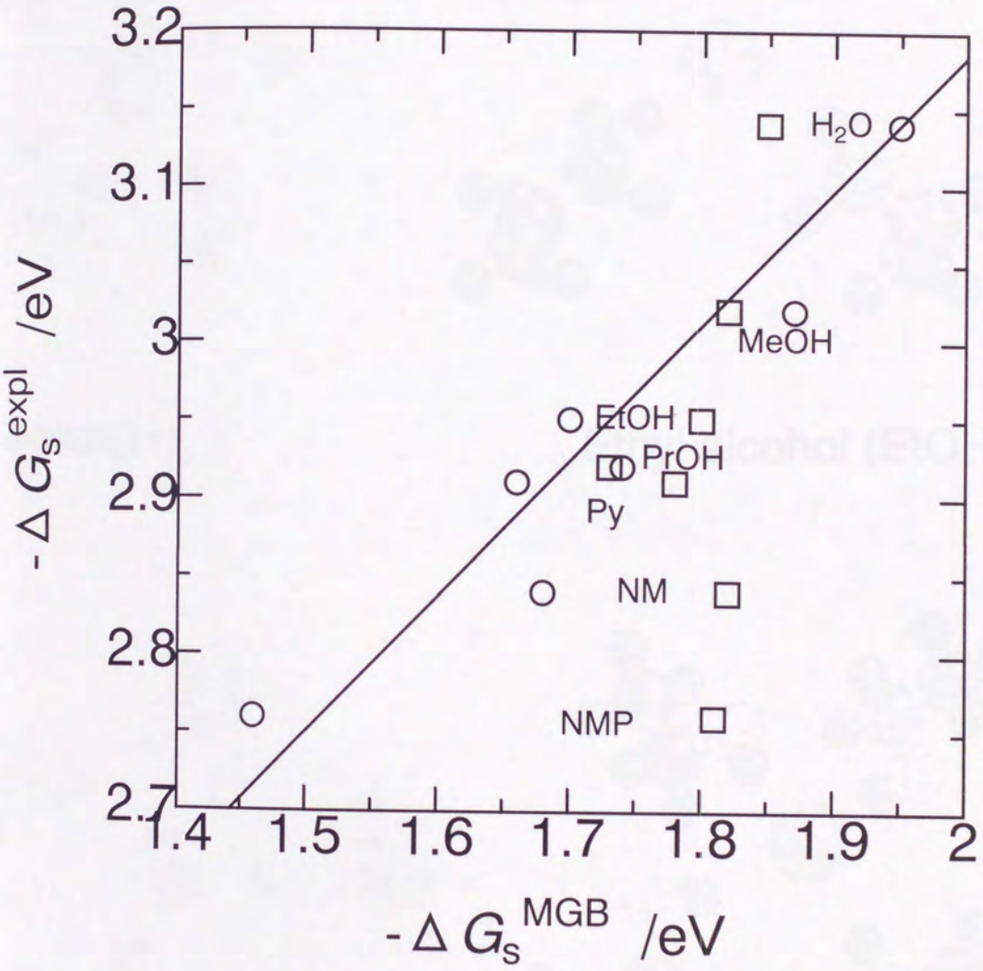

Fig. 4.4.2. Correlation of the solvation energy calculated by MOMGB using the cluster (○) and the bromide anion only (□) with experimental one for bromide anion in various solvents.

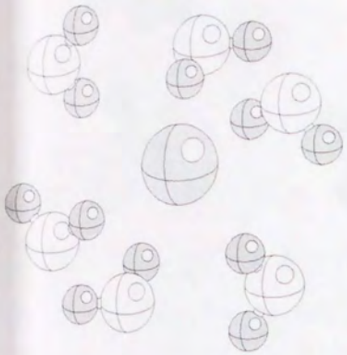

Water(H_2O)

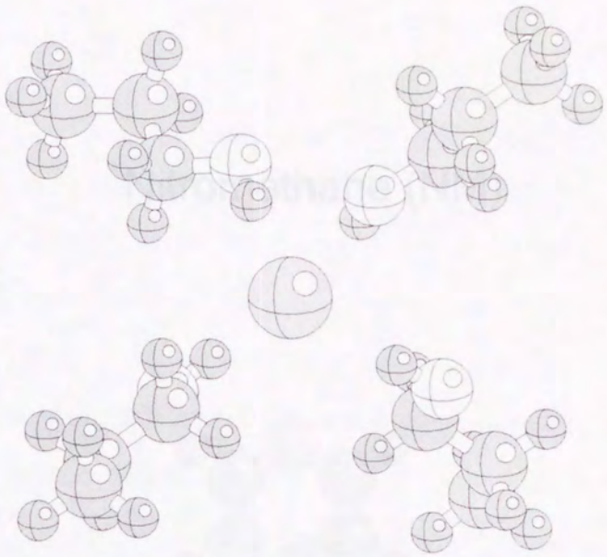

Ethyl alcohol (EtOH)

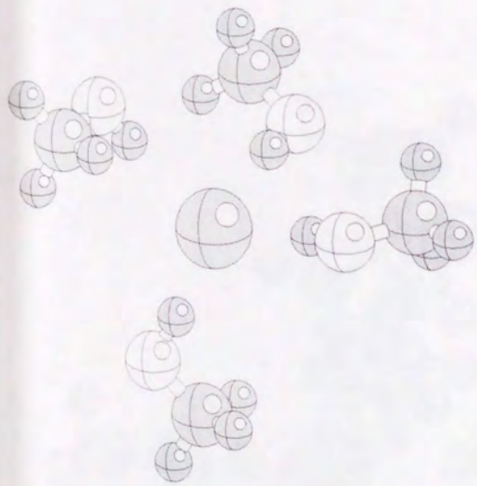

Methyl alcohol (MeOH)

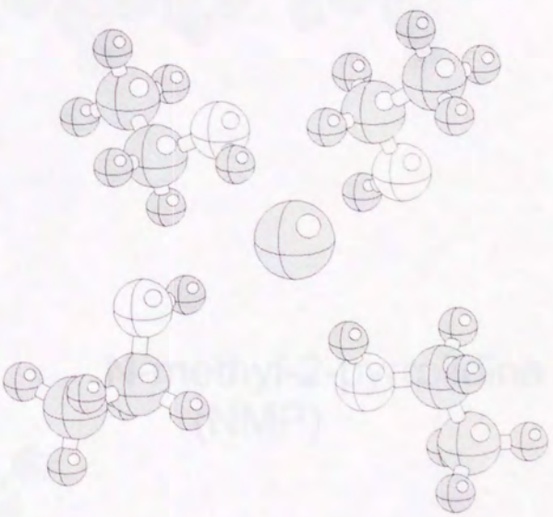

Propyl alcohol (PrOH)

Protic Solvents

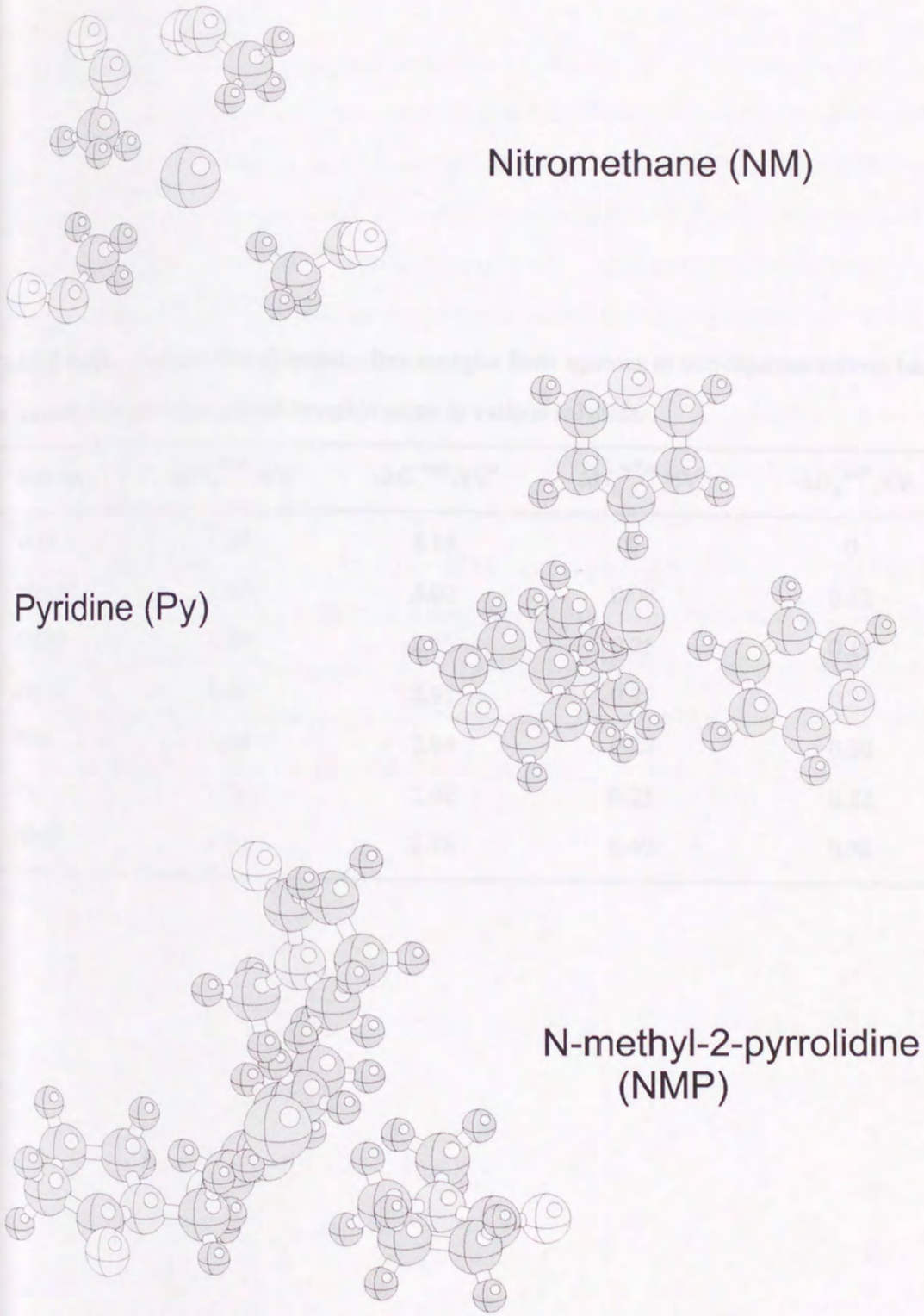

Fig. 4.4.3. The cluster model of Brimide anion coordinated by some solvent molecules.

TABLE 4.4.3. Calculation of transfer free energies from aqueous to non-aqueous solvent based on the solvation free energies of bromide anion in various solvents.

Solvent	$-\Delta G_s^{MGB}$ /eV	$-\Delta G_s^{expl}$ /eV[a]	$-\Delta G_{tr}^{MGB}$ /eV	$-\Delta G_{tr}^{expl}$ /eV
H_2O	1.95	3.14	0	0
MeOH	1.87	3.02	0.08	0.12
EtOH	1.70	2.95	0.25	0.19
PrOH	1.66	2.91	0.29	0.23
NM	1.68	2.84	0.27	0.30
Py	1.74	2.92	0.21	0.22
NMP	1.46	2.76	0.49	0.38

Ionization potential in solution.

Ionization potential of bromide anion in solution is estimated by the same manner as the case of the alkoxide anion, i.e. using the eigen value of HOMO. The results calculated without the modeling of cluster are listed in Table 4.4.4. and plotted in Fig.4.4.4. And, the results by MOMGB calculation using the cluster model which using the cluster insists of bromide anion and some solvent molecules are listed in Table 4.4.5. and plotted in Fig. 4.4.5. Similar to the solvation free energy, the values calculated using the cluster model are better agreement with the experimental one than the values calculated for the bromide anion only.

An electron is removed from HOMO level of the solvated molecule in the ionization process and thus the ionization potential is due to how the eigen vectors on HOMO level are distributed. All the eigen vector of HOMO level of the bromide anion is localized on the bromide atom but the eigen vectors of HOMO are spread not only the bromide atom but also the atoms of the coordibated solvents when the cluster is considered in MOMGB calculation. However, the calculated values of a bromide anion in NMP using the cluster is smaller than that obtained for the bromide anion only. This result indicates that the cluster model is necessary for the calculation of the ionization potentials of bromide anion, when the solute-solvent interaction is weak.

TABLE 4.4.4. Calculation of HOMO's eigen value of Bromide anion in various solvents.

Solvent	ε_r	$-\varepsilon_{HOMO}^{MGB}$ /eV	E_t^{expl} /eV[b]
H_2O	78.30	7.30	7.79
MeOH	32.66	7.23	7.61
EtOH	24.55	7.19	7.32
PrOH	20.45	7.16	7.36
NM	35.87	7.24	7.16
Py	12.91	7.06	6.55
NMP	32.20	7.23	6.27

b ref. [1-5]

TABLE 4.4.5. Calculation of HOMO's eigen value of Bromide anion in various solvents by MOMGB using the cluster.

Solvent	$-\varepsilon_{HOMO}^{MGB}$ (cluster) /eV	E_t^{expl} /eV
H_2O	8.37	7.79
MeOH	7.94	7.61
EtOH	7.75	7.32
PrOH	7.75	7.36
NM	7.84	7.16
Py	7.28	6.55
NMP	7.06	6.27

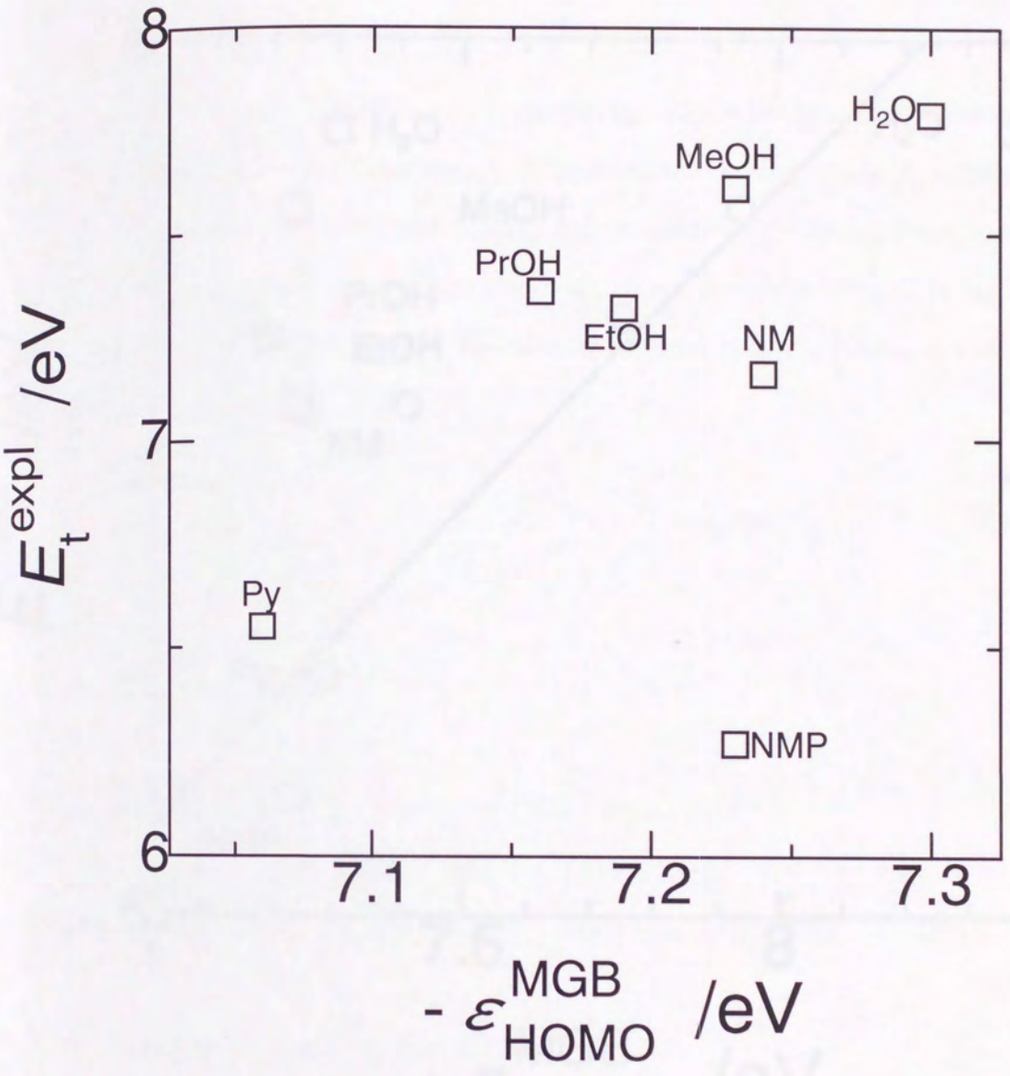

Fig.4.4.4. Correlation of the ionization potential calculated by MOMGB with experimental one for bromide anion in various solvents.

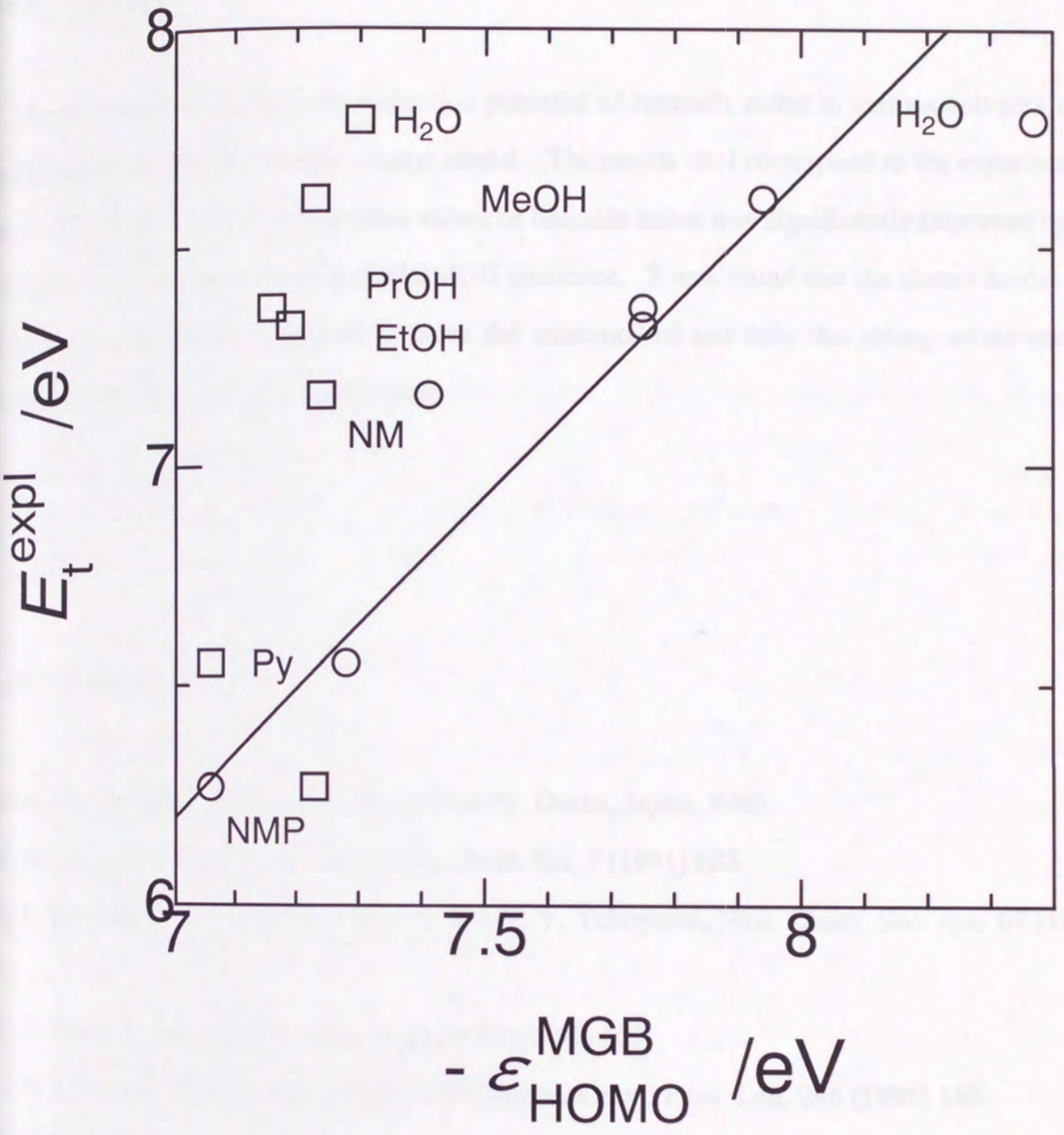

Fig. 4.4.5. Correlation of the ionization potential calculated by MOMGB using the cluster (○) and the bromide anion only (□) with experimental one for bromide anion in various solvents.

4.4.4. Conclusion

The solvation free energy and ionization potential of bromide anion in various solvents were calculated by MOMGB using the cluster model. The results well correspond to the experimental ones. The calculation of the solvation values of bromide anion was significantly improved by the introduction of the cluster model in MOMGB treatment. It was found that the cluster model was effective for the systems including under the existence of not only the strong solute-solvent interaction but also the weak interaction.

4.4.5. References

[1] H. Tanida, Doctor's thesis, Osaka university, Osaka, Japan, 1995.

[2] H. Tanida, I Watanabe, Y. Yokoyama, Anal. Sci. 7 (1991) 683.

[3] I. Watanabe, H. Tanida, K. Maya, S. Ikeda, Y. Yokoyama, Bull. Chem. Soc. Jpn. 67 (1994) 39.

[4] H. Tanida, I. Watanabe, J. Mol. Liquids 65 (1995) 409.

[5] N. Takahashi, K. Sakai, H. Tanida, I. Watanabe, Chem. Phys. Lett. 246 (1995) 183.

[6] H. Tanida, H. Sakane, I. Watanabe, Y. Yokoyama, Chem. Lett. (1993) 1647.

[7] H. Tanida, H. Sakane, I. Watanabe, J. Chem. Soc. Dalton Trans. (1994) 2321.

[8] I. Watanabe, H. Tanida, Anal. Sci. 11 (1995) 525.

Acknowledgement

The author wishes to express his greatest gratitude to Professor Hitoshi Watarai for his kind suggestion and support in coordinating this work.

The author also would like to express his sincere thanks to Associate Professor Iwao Watanabe for his helpful discussion and encouragement.

The author wishes to Dr. Hajime Tanida, Ms. Kanna Sakai and Mr. Yasuo Ohga for their kind supply of the data of bromide anions, alkoxide anions and poly-cyclic aromatic hydrocarbons and guidance for the photoelectron emission spectroscopy.

The author is also grateful to many members of Watarai laboratory for their helpful advice and assistance.

Appendix

Appendix A. Poly-Aromatic Hydrocarbons (PAHs)

Benzene

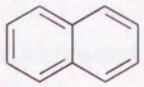

Naphthalene

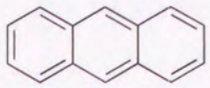

Anthracene

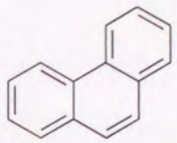

Phenanthrene

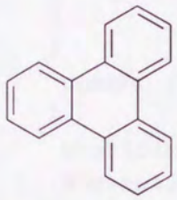

Triphenylene

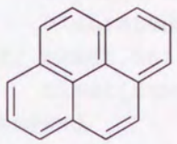

Pyrene

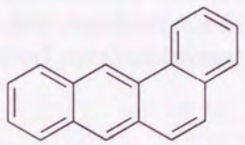

Benz[a]anthracene

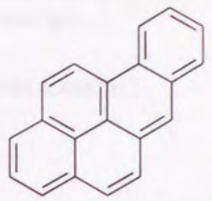

Benzo[a]pyrene

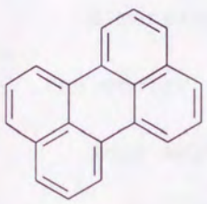

Perylene

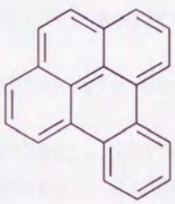

Benzo[e]pyrene

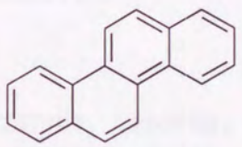

Chysene

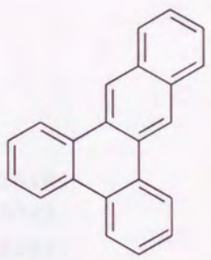

Benzo[b]triphenylene

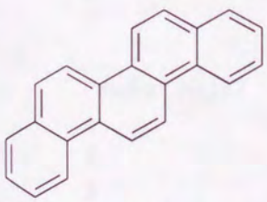

Benzo[e]chrysene

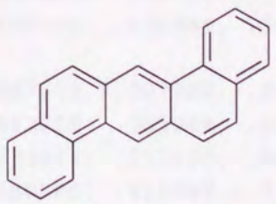

Dibenz[a,h] anthracene

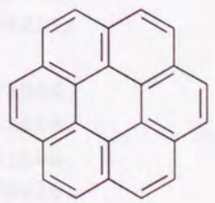

Coronene

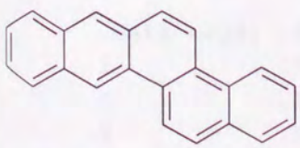

Benzo[b]chrysene

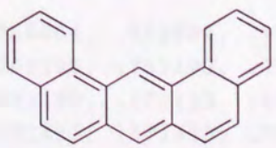

Dibenz[a,j]anthracene

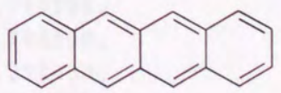

Napthsene

Appendix B. MOMGB program (determination of MGB radius, L_i)

```
      subroutine surfdist(coord)
      include 'sizes.h'
      implicit double precision (a-h,o-z)
      common /keywrd/ keywrd
      common /mgb   / SurfD(numatm,80),C_sol,Emgb(numatm),
     1                Ra(numatm),Surfac(numatm),Lmgb(numatm,numatm),
     2                zeff(numatm),q(numatm), CiCk(numatm,numatm),
     3                DisLin(numatm,80),numSur(numatm,80)
      common /molkst/ numat,nat(numatm),nfirst(numatm),nmidle(numatm),
     1                nlast(numatm)
      character*80 keywrd
      dimension coord(3,*),waals(100)
      dimension DistX(numatm,numatm),DistY(numatm,numatm)
      dimension DistZ(numatm,numatm),Distij(numatm,numatm)
      dimension numSur(numatm,80)
      dimension CiCk(numatm,80)
      dimension DisLin(numatm,80)
      dimension segX(40), segY(40), segZ(40)
C
C  the vector of Surficity's Segment
C
      data segX/ .207709,-.207709,-.207709, .207709, .562618,
     1           .233044,-.233044,-.562618,-.562618,-.233044,
     2           .233044, .562618, .792686, .580286, .212399,
     3          -.212400,-.580286,-.792686,-.792686,-.580286,
     4          -.212399, .212400, .580286, .792686, .938211,
     5           .795377, .531454, .186622,-.186622,-.531454,
     6          -.795377,-.938211,-.938211,-.795377,-.531454,
     7          -.186621, .186622, .531454, .795377, .938211/
C
      data segY/ .207709, .207709,-.207709,-.207709, .233044,
     1           .562618, .562618, .233044,-.233044,-.562618,
     2          -.562618,-.233044, .212400, .580286, .792686,
     3           .792686, .580286, .212399,-.212400,-.580286,
     4          -.792686,-.792686,-.580286,-.212399, .186622,
     5           .531454, .795377, .938211, .938211, .795377,
     6           .531454, .186622,-.186622,-.531454,-.795377,
     7          -.938211,-.938211,-.795377,-.531454,-.186622/
C
      data segZ/ .955884, .955884, .955884, .955884, .793190,
     1           .793190, .793190, .793190, .793190, .793190,
     2           .793190, .793190, .571433, .571433, .571433,
     3           .571433, .571433, .571433, .571433, .571433,
     4           .571433, .571433, .571433, .571433, .291431,
     5           .291431, .291431, .291431, .291431, .291431,
     6           .291431, .291431, .291431, .291431, .291431,
```

```
     7          .291431, .291431, .291431, .291431, .291431/
C
C      VAN DER WAALS RADII A LA BONDI, JPC 68 (1964) 441.
C
      data waals/
     1 1.20,                                                    0.00,
     2 1.82,0.00,                        0.00,1.70,1.55,1.52,1.47 ,1.54,
     3 2.27,1.73,                        2.50,2.10,1.80,1.80,1.75 ,1.88,
     4 2.75,0.00,7*0.00,1.63,1.40,1.39, 2.40,2.10,1.85,1.90,1.85 ,2.02,
     5 0.00,0.00,7*0.00,1.63,1.72,1.58, 2.50,2.20,2.10,2.06,1.98 ,2.60,
     6  46*0.00/
C  save
C
C  Seach segment - solvent distance
C
C  "Ra(i)" is the Radius of i_th atom,
C  "SurfD(i,j)" is the distance from the center of i_th atom
C    to j_th segment.
C
      if (INDEX(keywrd,'RSOL=').ne.0) then
         Rsol=reada(keywrd, index(keywrd,'RSOL='))
        else Rsol=1.4d0
       endif
C
      do 20 i=1,numat
        Ra(i)=waals(nat(i))
        do 10 k=1,80
          SurfD(i,k)=Ra(i)
10      continue
20    continue
C
      do 50 i=2,numat
        do 40 j=1,(i-1)
          DistX(i,j)=coord(1,i)-coord(1,j)
          DX=DistX(i,j)
          DistY(i,j)=coord(2,i)-coord(2,j)
          DY=DistY(i,j)
          DistZ(i,j)=coord(3,i)-coord(3,j)
          DZ=DistZ(i,j)
          Distij(i,j)=sqrt(DX*DX+DY*DY+DZ*DZ)
40      continue
50    continue
      do 70 i=1,numat
         DistX(i,i)=0.d0
         DistY(i,i)=0.d0
         DistZ(i,i)=0.d0
         Distij(i,i)=0.d0
         do 60 j=(i+1),numat
            DistX(i,j)=-DistX(j,i)
```

```
          DistY(i,j)=-DistY(j,i)
          DistZ(i,j)=-DistZ(j,i)
          Distij(i,j)=Distij(j,i)
60      continue
70     continue
C
C  Seaching Distance to Solvent in direction to Segment's Vector.
C
      do 130 i=1,numat
        do 120 j=1,40
          numSur(i,j)=i
          numSur(i,j+40)=i
          CiCk(i,j)=0.d0
          CiCk(i,j+40)=0.d0
          DisLin(i,j)=0.d0
          DisLin(i,j+40)=0.d0
          do 110 k=1,numat
            if (k.eq.i) goto 110
            Xik=DistX(i,k)
            Yik=DistY(i,k)
            Zik=DistZ(i,k)
            Dij=Distij(i,k)
            Dis2_1=Xik*Xik+Yik*Yik+Zik*Zik
     1                   -(segX(j)*Xik+segY(j)*Yik+segZ(j)*Zik)**2
            Dis2_2=Dis2_1
            cTheta=(segX(j)*Xik+segY(j)*Yik++segZ(j)*Zik)/Dij
            RDis21=sqrt(Dis2_1)
            RDis22=sqrt(Dis2_2)
            if ( (RDis21.le.Ra(k)) .and.
     1           (CiCk(i,j).le.Distij(i,k)) .and. (ctheta.ge.0) ) then
              numSur(i,j)=k
              CiCk(i,j)=Distij(i,k)
              DisLin(i,j)=RDis21
            endif
            if ( (RDis22.le.Ra(k)) .and.
     1           (CiCk(i,j+40).le.Distij(i,k)) .and. (ctheta.lt.0)) then
              numSur(i,j+40)=k
              CiCk(i,j+40)=Distij(i,k)
              DisLin(i,j+40)=RDis22
            endif
110         continue
120       continue
130     continue
      do 150 i=1,numat
        do 140 j=1,80
          SurfD(i,j)=sqrt( CiCk(i,j)**2-DisLin(i,j)**2 ) +
     1                 sqrt( Ra(numSur(i,j))**2 - DisLin(i,j)**2 )
       if (SurfD(i,j).lt.Ra(i)) then
       SurfD(i,j)=Ra(i)
```

```
      endif
C      write(6,'(''i, SurfD,CiCk,DisLin,numSur,Ra = '',I5,F12.5,F12.5,
C     1F12.5,I5,F12.5)')i,SurfD(i,j),CiCk(i,j),DisLin(i,j),numSur(i,j),
C     2Ra(numSur(i,j))
140       continue
150   continue
C
C
C  Calculate "Surfac"
C
      do 410 i=1,numat
         Surfac(i)=0.d0
410   continue
C
      do 440 i=1,numat
        do 430 j=1,80
C
C    Surfac(i) : i th atom's 1/r (r:temporary radius)
C     1/r = 1/80*( 1/r1 + 1/r2+ .... )
C
          Surfac(i)=Surfac(i)+(0.0125d0/SurfD(i,j))
430     continue
440   continue
      do 470 i=1,numat
C
C    Surfac(i) : 1/r -> r
C
        Surfac(i)=1.d0/Surfac(i)
        Lmgb(i,i)=Surfac(i)*2.d0
470   continue
      do 490 i=2,numat
         do 480 j=1,(i-1)
         Lmgb(i,j)=sqrt(Distij(i,j)**2
     1              +0.25d0*( ( Surfac(i)+Surfac(j) )**2 ) )
         Lmgb(j,i)=Lmgb(i,j)
480      continue
490   continue
      return
      end


      subroutine MGBorn(niter)
      implicit double precision (a-h,o-z)
      include 'sizes.h'
      common /optim / imp,imp0,lec,iprt
      common /densty/ p(mpack)
      common /geom  / geo(3,numatm)
      common /molkst/ numat,nat(numatm),nfirst(numatm),nmidle(numatm),
```

```
     1               nlast(numatm)
      common /keywrd/ keywrd
      common /mgb    / SurfD(numatm,80),Cmgb,C_sol,Emgb(numatm),
     1                 Ra(numatm),Surfac(numatm),LMgb(numatm,numatm),
     2                 zeff(numatm),q(numatm)
      character*241 keywrd
      dimension zhelp(100),coord(3,numatm)
      data zhelp/
     1 1.,                                                    2.,
     2 1., 2.,                                3., 4., 5., 6., 7., 8.,
     3 1., 2.,                                3., 4., 5., 6., 7., 8.,
     4 1., 2.,          10*2.,                3., 4., 5., 6., 7., 8.,
     5 1., 2.,          10*2.,                3., 4., 5., 6., 7., 8.,
     6 1., 2.,          24*2.,                3., 4., 5., 6., 7., 8.,
     7 1., 2.,          12*2./
    save
C
C   Define various Constant for Solvation Energy Calculation
C      "E0" is dielectric constant in vacuum,
C      "elect" is Elementary Electric Charge,
C      "pi" is circular constant.
C
       E0=8.85419d-12
       elect=1.60219d-19
       pi=3.141592654d0
       K=0
       Cmgb=0.d0
C
C  Read Rerative Permittivity of Solvent, Er
C
       if (INDEX(keywrd,'ER=').ne.0) then
         permit=reada(keywrd, index(keywrd,'ER='))
        else permit=78.3d0
       endif
C
C  Calculate Coefficient for Solvation Energy, C_sol
C
      C_sol=1-(1/permit)
C
C  Seach segment - solvent distance
C
C  "numij" is the sum of i-j interaction.
C
C      numij=numat*(numat-1)/2
C
C  CALCULATE THE 'EFFECTIVE' NUCLEAR CHARGE--I.E. VALENCE PROTONS
C
      do 10 i=1,numat
10    zeff(i)=zhelp(nat(i))
```

```
C
C  CALCULATE ATOMIC CHARGES
C
      do 30 i=1,numat
         Emgb(i)=0.d0
         q(i)=zeff(i)
         do 20 j=nfirst(i),nlast(i)
            k=k+j
20          q(i)=q(i)-p(k)
30    continue
C
C
C
      if(sqrt(float(niter)).ne.int(sqrt(float(niter)))) go to 100
      call gmetry(geo,coord)
      call surfdist(coord)
100   continue
      do 140 i=1,numat
C      jp=i+1
      do 120 j=1,i
      Emgb(i)=Emgb(i)+q(j)/LMgb(i,j)
120   Cmgb=Cmgb-7.1983d0*C_sol*zeff(j)*q(i)/LMgb(i,j)
      do 130 k=(i+1),numat
      Emgb(i)=Emgb(i)+q(k)/LMgb(k,i)
130   Cmgb=Cmgb-7.1983d0*C_sol*zeff(k)*q(i)/LMgb(k,i)
140   continue
      do 200 i=1,numat
         Emgb(i)=14.3966d0*C_sol*Emgb(i)
200   continue
      return
      end
```